7. SITE 395[1]

Shipboard Scientific Party[2]

HOLE 395A[3]

Date reoccupied: 2 June 1986, 1200 L

Date departed: 11 June 1986, 1930 L

Time on hole: 9 days, 7.5 hr (includes 4 hr, 40 min, at Hole 395C to measure temperatures in the sedimentary section)

Position: 22°45.35′N, 46°04.9′W

Water depth (sea level; corrected m, echo-sounding): 4490.2

Water depth (rig floor; corrected m; echo-sounding): 4501.3

Bottom felt (m, drill pipe): 4494

Distance between rig floor and sea level (m): 11.1

HOLE 395C

Date occupied: 7 June 1986, 1800 L

Date departed: 7 June 1986, 2240 L

Time on hole: 4 hr, 40 min

Position: 22°45.5′N, 46°04.9′W

Water depth (sea level; corrected m, echo-sounding): 4490.2

Water depth (rig floor; corrected m, echo-sounding): 4501.3

Bottom felt (m, drill pipe): 4494

Distance between rig floor and sea level (m): 11.1

Penetration (m): 70 (washed to 70 mbsf to measure temperatures in sedimentary section)

Number of cores: 0

Total length of cored section (m): 0

Total core recovered (m): 0

Principal results: *JOIDES Resolution* arrived at Site 395 on 2 June, and Hole 395A was reentered at 1019 hr on 3 June for a 9-day program of logging and downhole experiments. Immediately after reentry, equilibrium temperatures through the 112 m of casing were measured, verifying that ocean-bottom water continues to flow down the hole at a rate on the order of 1000 L/hr. A 45-mL sample of borehole fluid was taken at 544 mbsf. The pipe was run slowly and without circulation or rotation, for minimal disturbance to borehole temperatures, to hole bottom at 606 mbsf. Next, the pipe was held at the bottom of the hole, and temperatures as close to equilibrium as possible were continuously logged inside the pipe with the BGR temperature probe developed by the Federal Institute for Geosciences and Natural Resources, Federal Republic of Germany. The results indicate that the downhole flow extends to about 400 mbsf and that a linear, conductive gradient prevails in the deeper section of basement.

We then pulled up the pipe within the 112 m of casing and successfully logged the 494 m of open hole through basement during the next 4 days with the following tools (in order of deployment): Schlumberger GST-ACT-NGT (neutron activation), German magnetometer (vertical field only), Schlumberger DIL-LSS-SFL-GR-CALI (sonic and resistivity), German magnetic susceptibility, LDGO multichannel sonic, Japanese magnetometer, large-scale resistivity, and Schlumberger LDT-CNT-G-NGT (lithodensity plus inclinometer). The pipe was then pulled out of the hole and offset 110 m northwest, where the background geothermal gradient was measured in the sediments of Hole 395C. The pipe was pulled to the surface by 1200 hr 9 June, and a straddle packer was installed in the bottom-hole assembly. After television-sonar verification of mud-line depth and after reentry at 0700 hr 10 June, the packer was successfully set at 396 and 536 mbsf for bulk permeability measurements over the lowermost 210 and 80 m of open hole. The allotted 8 days for logging Hole 395A had expired when the packer go-devil lodged in the pipe on retrieval, and operations at Site 395 were terminated when the bit was pulled on deck by 1930 hr, 11 June.

All the logs were affected to some degree by irregular hole conditions, but preliminary interpretation of the log data suggests the following results. In the deep part of the hole, compressional sonic velocities are 5.0–5.5 km/s and shear-wave velocities are about 3 km/s, but cycle skipping mars the data from the shallow section. Neutron porosities are about 10%–20%, and densities are 2.2–2.8 g/cm^3. Resistivities are about 10–100 Ωm in the upper 400 m of basement, increasing to about 200 Ωm in the deepest 100 m. The magnetic data clearly show a reversal about 150 m into basement. Several distinct units, roughly 10–50 m, thick are apparent in the logs, and the basement is presumably heterogeneous over similar vertical scales. None of the logs shows any evidence of the cement plug that disappeared into the formation during DSDP Leg 45. Most of the section is quite permeable, and bulk permeabilities of the upper 300 m, lowermost 210 m, and lowermost 80 m are orders of magnitude higher than the extremely low value measured below 583 mbsf during DSDP Leg 78B.

The only tools on board Leg 109 that time did not allow us to run were the borehole televiewer and the Schlumberger dual laterolog. Overall, Leg 109 was successful in establishing Hole 395A as a

[1] Bryan, W. B., Juteau, T., et al., 1988. *Proc. ODP, Init. Repts. (Pt. A)*, 109: College Station, TX (Ocean Drilling Program).

[2] Wilfred B. Bryan (Co-Chief Scientist), Department of Geology and Geophysics, Woods Hole Oceanographic Institution, Woods Hole, MA 02543; Thierry Juteau (Co-Chief Scientist), Laboratoire de Pétrologie, Université de Bretagne Occidentale, 6 Avenue Le Gorgeu, 29287 Brest, France; Andrew C. Adamson (ODP Staff Scientist), Ocean Drilling Program, Texas A&M University, College Station, TX 77843; Laurie K. Autio, Department of Geology and Geography, Morrill Science Center, University of Massachusetts, Amherst, MA 01003; Keir Becker, R.S.M.A.S., Division of Marine Geology and Geophysics, University of Miami, 4600 Rickenbacker Causeway, Miami, FL 33149; M. Mansour Bina, Laboratoire de Géomagnetisme, Université Pierre et Marie Curie, 4 Avenue de Neptune, 94107 St. Maur des Fosses, France; Jean-Philippe Eissen, O.R.S.T.O.M., B.P. A5, Noumea, New Caledonia (current address: O.R.S.T.O.M., IFREMER, BP 337, 2273 Brest Cedex, France); Toshitsugu Fujii, Earthquake Research Institute, University of Tokyo, 1-1-1 Yayoi, Bunkyo-ku, Tokyo 113, Japan; Timothy L. Grove, Department of Earth, Atmospheric and Planetary Sciences, Massachusetts Institute of Technology, Cambridge, MA 02139; Yozo Hamano, Earthquake Research Institute, University of Tokyo, 1-1-1 Yayoi, Bunkyo-ku, Tokyo 113, Japan; Rejean Hebert, Departement de Géologie, Université Laval, Quebec G1K 7P4, Canada; Stephen C. Komor, Bureau of Mines, Avondale Research Center, 4900 LaSalle Road, Avondale, MD 20782 (current address: Department of Geology and Geophysics, University of Wisconsin, Madison, WI 53706); Johannes Kopietz, Bundesanstalt für Geowissenschaften und Rohstoffe, Stilleweg 2, D-3000 Hannover 51, Federal Republic of Germany; Kristian Krammer, Institut für Geophysik, Universität München, Theresienstrasse 41, D-8000 München 2, Federal Republic of Germany; Michel Loubet, Laboratoire de Mineralogie, Université Paul Sabatier, 38 Rue des 36 Ponts, 31400 Toulouse, France; Daniel Moos, Borehole Research Group, Lamont-Doherty Geological Observatory, Columbia University, Palisades, NY 10964; Hugh G. Richards, Department of Geology, The University, Newcastle upon Tyne NE1 7RU, United Kingdom.

[3] Operations at Hole 395A were devoted entirely to logging the basement section. Hole 395A penetrates 93 m of sediment and 571 m of basement.

geophysical reference section, complementing results at Holes 418A and 504B.

BACKGROUND AND OBJECTIVES

One of the major objectives of the JOIDES Downhole Measurements Panel (DMP) for the Ocean Drilling Program is to assemble a reference suite of borehole geophysical data from deep holes drilled into the oceanic basement. DMP has three general purposes for logging basement holes:

1. Determining variations in the geophysical properties of the oceanic crust vs. depth, age, and spreading rate.
2. Determining the underlying causes of these variations through comparisons with the core and geological history of each site.
3. Providing ground truth and a geological basis for the interpretation of surface geophysical data.

In principle, this requires that a small number of deep basement holes, representing a spectrum of ages and spreading rates, be studied with similar, comprehensive suites of state-of-the-art tools. To date, such studies have been attempted in three holes deeper than 500 m into basement: Holes 395A, 418A, and 504B (Fig. 1).

The most notable of these studies was conducted in Hole 504B over the course of DSDP Legs 69, 70, 83, and 92, and during ODP Leg 111. The results from Leg 69 through Leg 92 have shown the following in Hole 504B:

1. Seismic layers 2A, 2B, and 2C correspond respectively to open-pillow lavas and rubble, partly sealed pillow lavas, and sheeted dikes.
2. The velocity structure of the crust is controlled not by petrology but by variations in porosity with depth.
3. The formation porosity decreases from an average of 10%–15% in the upper 600 m of crust (layers 2A and 2B) to 1%–2% in the dikes at the base of the hole (layer 2C).
4. The permeability of the crust decreases by 2–3 orders of magnitude with depth in the upper 1 km of crust, consistent with the tenfold decrease in porosity.
5. Nonhydrostatic pore pressures developed and were maintained in the uppermost basement and are presumably related to convection of pore fluids. (Anderson, Honnorez, et al., 1982; Cann, Langseth, Honnorez, Von Herzen, White, et al., 1983; Anderson, Honnorez, et al, 1985; Anderson and Zoback, 1982; Becker, Von Herzen, Francis, et al., 1982; Becker et al., 1983b; Anderson et al., 1985.)

Although the logging results from Hole 504B are quite convincing, generalizations should not be drawn from this single well-studied example. In 1984–85, the DMP proposed that Holes 395A and 418A in the Atlantic be logged early during the Ocean Drilling Program, to complement the results from Hole 504B. During Leg 102, Hole 418A was logged successfully and was reopened for future drilling (Salisbury, Scott, Auroux, et al., 1986). With the strong endorsement of both DMP and the Lithosphere Panel, logging Hole 395A was the top-priority contingency plan for Leg 109; when efforts at Hole 648B were terminated, Leg 109 devoted 8 days to logging Hole 395A.

Hole 395A had been drilled during Leg 45 in 1975–76 (Melson, Rabinowitz, et al., 1978) in a sediment pond on 7.3-m.y.-old crust directly west of the location later chosen for Site 648 on the Mid-Atlantic Ridge (Fig. 2). Leg 45 cored through 93 m of sediment and 571 m of basement, leaving Hole 395A cased to a depth of 112 mbsf. Some logging was attempted during Leg 45, but it was quickly terminated when a hydrophone was lost in the hole.

Leg 78B returned to Hole 395A in 1981 to log the hole but suffered from many instrumental and operational problems (Hyndman, Salisbury, et al., 1984). Because of these problems, Leg 78B returned with no porosity data from Hole 395A and only marginal geothermal, density, velocity, resistivity, and permeability data (Fig. 3). During operations, Leg 78B encountered an impenetrable bridge 55 m above the bottom of the Leg 45 hole and released a bit above this bridge.

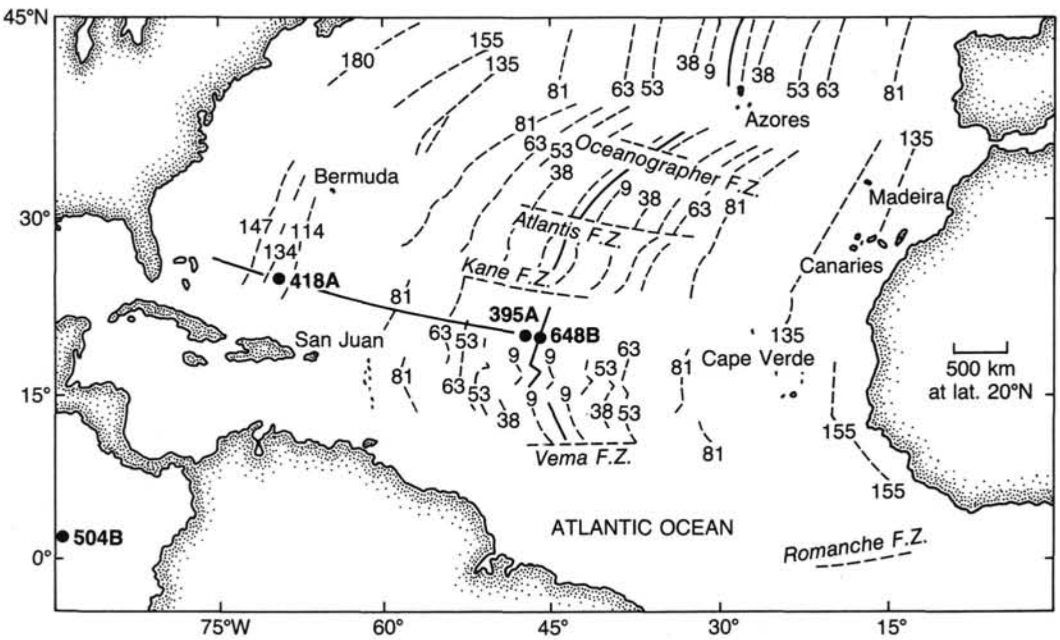

Figure 1. Location of Holes 395A, 418A, 504B, and 648B. Dashed lines show age of crust in Ma, deduced from magnetic anomalies. After Salisbury and Hyndman (1984).

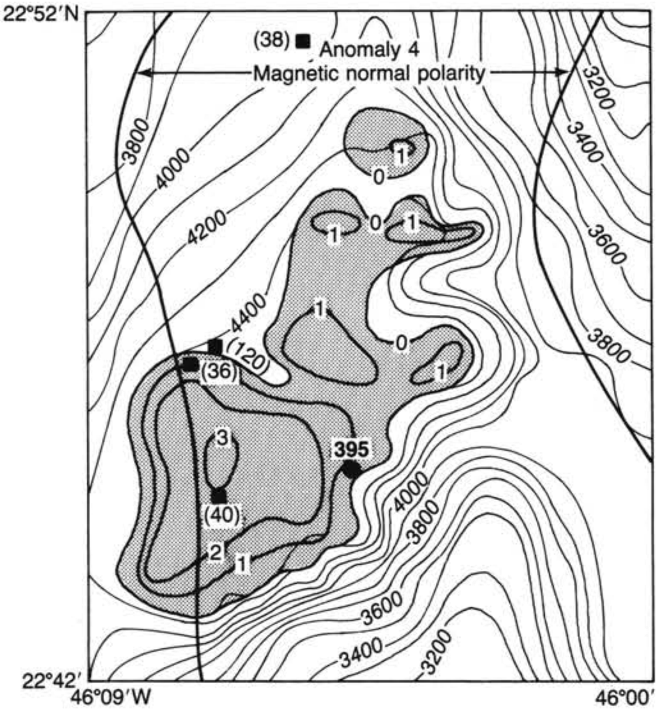

Figure 2. Bathymetry in corrected meters and sediment isopachs in seconds of two-way traveltime near Site 395. Shown also are boundaries of magnetic anomaly 4 and heat-flow stations (solid squares), with values in mW/m^2. From Salisbury and Hyndman (1984).

For Leg 109, DMP endorsed an 8-day return logging program in Hole 395A, specifically hoping to accomplish the following:

1. Determine the *in-situ* velocity structure in young Atlantic crust. Is layer 2A present in the upper levels of Hole 395A?
2. Determine the variation of porosity with depth in Hole 395A. Does the porosity decrease with age and depth in response to alteration?
3. Determine the permeability of young Atlantic crust. Does the permeability decrease with depth and how is it related to porosity?
4. Determine the temperature profiles in the hole and in the sediments at Site 395 to verify whether heat transfer occurs by conduction and/or by convection.
5. Assess whether or not the underpressures and downhole flow of ocean-bottom water observed during Leg 78B still persist.
6. Resample and analyze the chemistry of borehole fluids in partial equilibrium with pore fluids in young crust.
7. Refine the eruptive history of the layer 2 extrusive pile from variations in magnetic susceptibility and NRM intensity, inclination, and declination.

The specific experiments and tools planned for Hole 395A during Leg 109 included the following:

1. Conventional logging tools (Schlumberger): long-spaced sonic, dual induction, spherically focused laterolog, dual laterolog, compensated gamma density, compensated neutron porosity, caliper, spectral gamma ray, and neutron activation (elemental abundances).
2. Multichannel sonic logging (LDGO) to determine the velocities of compressional, shear, and Stoneley waves and the propagation characteristics of the section.
3. Borehole televiewer (LDGO) to observe mesoscopic features, such as pillows, fractures, and dikes in the well bore, and to determine the orientation of *in-situ* stresses from breakouts.
4. Large-scale resistivity experiment (Miami University) to determine the bulk porosity of the crust.
5. Packer (Miami University) test to determine the permeability of the upper levels of basement.
6. Three-axis magnetometer and magnetic-susceptibility tools (German) to determine the variation of magnetic susceptibility and natural remanent magnetization (NRM) intensity, inclination, and declination with depth and alteration. A Japanese-made three-axis magnetometer intended for Leg 111 was completed in time for use on Leg 109 as a backup to the German-made magnetometer.
7. High-resolution temperature tool (German) to measure the borehole temperature profile.
8. Temperature/water sampler (ODP) to measure equilibrium borehole temperatures and sample equilibrium borehole fluids simultaneously.
9. Advanced-piston-core (APC)–temperature tool (ODP/WHOI) to determine the geothermal gradient in the sediments adjacent to Hole 395A.

Early on Leg 109, we formulated a detailed 8-day logging plan for Hole 395A, which reflects both scientific and operational priorities. This plan is included here as Table 1, for comparison with Table 2 of the "Operations" section (this chapter), which shows the actual logs run in Hole 395A in order of deployment during Leg 109. Time allowed all but one of the recommended tools (borehole televiewer) to be run in Hole 395A. Overall, Leg 109 was successful in logging Hole 395A, thereby establishing a third geophysical reference section to complement results from Holes 418A and 504B.

OPERATIONS

This section summarizes the scientific operations at Site 395. Table 2 gives a detailed breakdown of the time spent for each measurement, and Figure 4 shows the depths over which the measurements were made and provides a preliminary estimate of the quality of the results.

Operational Summary

Leg 109 arrived at Site 395 at about 1200 hr on 2 June 1986 and dropped a beacon at 1209 hr. After solving some problems with reentry tools, we reentered Hole 395A at 1019 hr, 3 June. During the next day, pipe was run slowly down the hole without rotation or circulation. Two pauses were made during this pipe run to measure undisturbed temperatures ahead of the bit, using ODP tools on a wire rope. The first lowering was made to the bottom of casing, where accurate temperature measurements were critical in determining the flow rate of ocean-bottom water down the hole. Station measurements were made at the seafloor and at 100.6, 109.2, and 118.8 mbsf. The second lowering was made deep in the hole, and although the temperature recorders failed, a 45-mL sample of borehole fluid was taken at 544.6 mbsf.

After running the bit to hole bottom at 5100 m below rig floor (mbrf) (still without circulation or rotation), we pulled the pipe back 14 m. The German BGR temperature probe was then run in the pipe to obtain a continuous equilibrium-state temperature profile. The presence of the pipe probably smoothed out small-scale temperature anomalies, but the general shape of the curve is quite good. At the conclusion of the temperature-log run, the pipe was pulled back and the bit positioned near the casing shoe at about 4600 mbrf.

The first open-hole log was the Schlumberger dual-induction long-spacing sonic/spherically focused laterolog/gamma/caliper (DIL/LSS/SFL/GR/CALI) logging combination. Although this

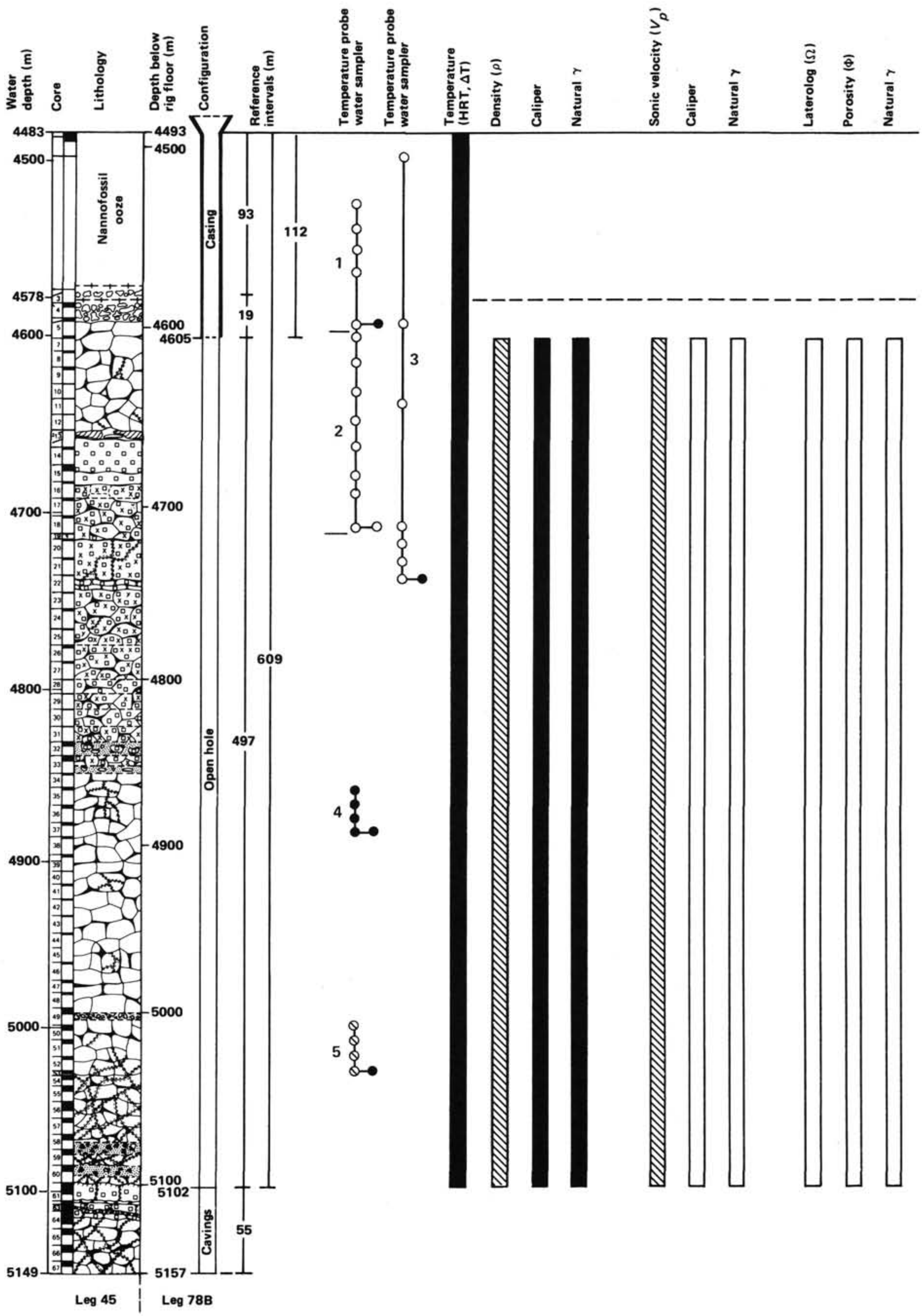

Figure 3. Operational summary of Leg 78B logging program in Hole 395A. From Hyndman, Salisbury, et al. (1984).

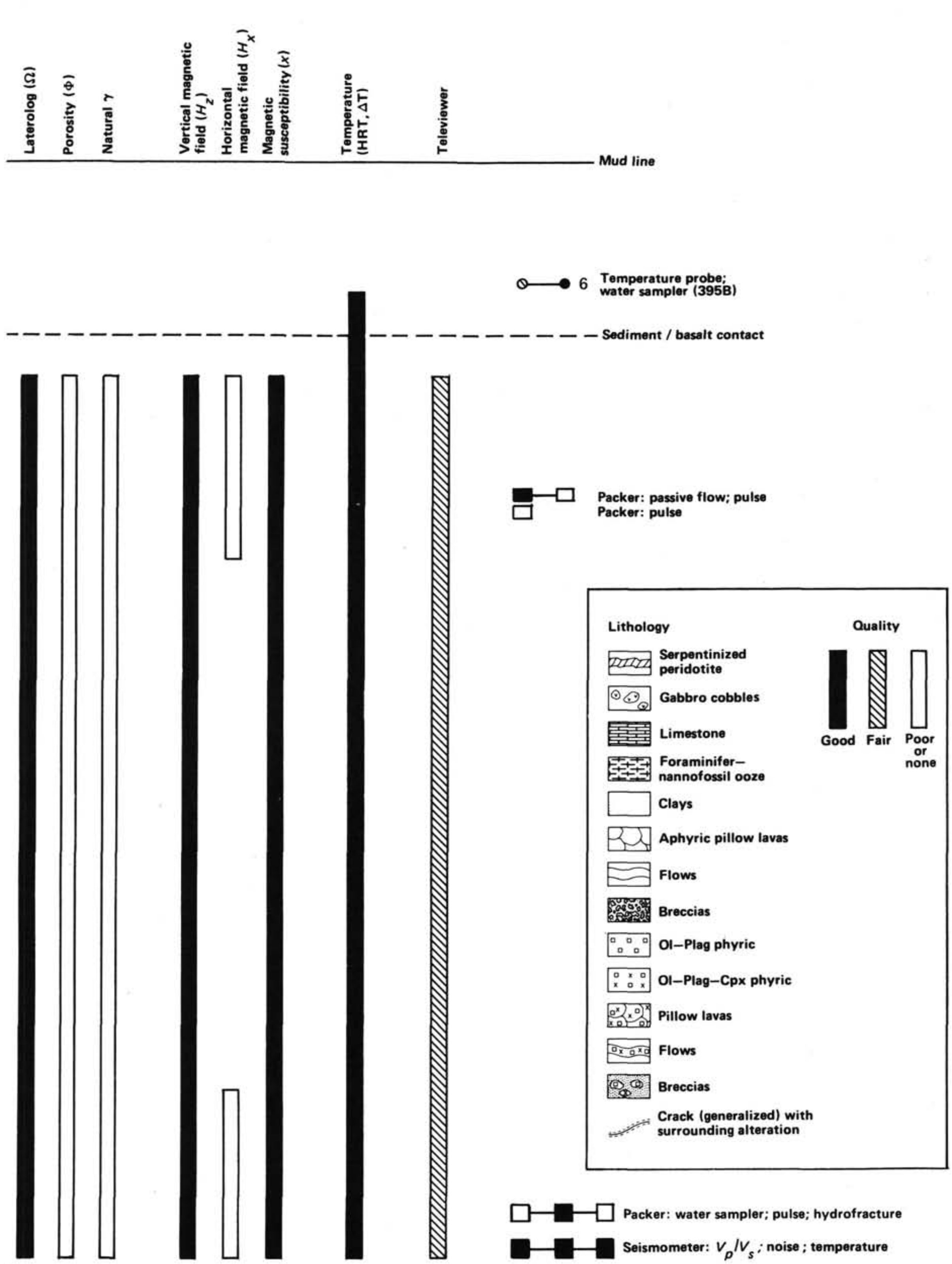

Figure 3 (continued).

tool worked perfectly running into the hole, an electronic component failed just as it exited the pipe, so we aborted the log.

We brought the tool to the surface and deployed the next Schlumberger logging tool, the aluminium-clay/gamma spectroscopy/natural gamma (GST/ACT/NGT) combination, designed to determine the concentrations of K, U, and Th from the spectrum of naturally emitted gamma rays, and Fe, Si, Ca, Al, S, H, and Cl from their activated spectra. The initial combination did not calibrate correctly at the surface, so the components were interchanged until a working combination could be found. The logging sonde was then run into the hole, and one full pass was completed. A second pass was attempted to im-

Table 1. Leg 109 logging plan for Hole 395A.[a]

Order	Log/experiment
First pipe trip (clean-out/logging bit)	
1	Temperatures to 4500 mbrf—ODP HPC/Uyeda tool.
2	Temperatures/water samples at about 5000 and 5050 mbrf—ODP Barnes/Uyeda + HPC tools.
Run pipe to touchdown. If this can be accomplished without circulation, leave pipe at bottom and run German T log in pipe. Hole conditioning, then pull bit back up into casing.	
3	Schlumberger DIL-LSS-SFL-GR-CALI.
4	Schlumberger GST-ACT-NGT.
5	Magnetometer, German.
6	Magnetic susceptibility.
7	Schlumberger LDT-CNT-G-NGT.
8	LDGO MCS + Japanese magnetometer.
9	LDGO BHTV.
10	Large-scale resistivity.
11	Flowmeter, if temperatures do not give flow rate.
?	(?—German T log, if not run already).
12	Offset to Hole 395C for sediment temperatures—ODP HPC tool, freefall.
Second pipe trip (packer in BHA)	
13	Temperature log—German (if not run already).
14	Packer—permeability tests.
15	If time allows, Schlumberger DLL and possible second attempts of any logging tools that may have failed the first time.

[a] 8-day logging program; revised 2 June 1986.

Table 2. Operational summary of logs and experiments run at Site 395 during Leg 109.

Order/start time		Log/experiment
First pipe trip (clean-out/logging bit); Hole 395A		
1	1800 3 June	Temperatures to 118 mbsf—ODP HPC tool; very good results.
2	0200 4 June	Temperature/water sample at 544 mbsf; ODP Barnes/Uyeda + HPC tools - 45 ml sample.
	0255 4 June	Ran pipe to touchdown at 5100 mbsf; hole was in excellent condition and pipe was left in hole to run German BGR temperature probe.
3	0640 4 June	BGR temperature log—very good results.
	1400 4 June	Hole conditioned for logging.
4	1900 4 June	Schlumberger LSS-DIL-SFL-GR-CALI malfunctioned; postponed.
5	0300 5 June	Schlumberger GST-ACT-NGT run into hole after solving problem with calibration results.
6	1600 5 June	GST-ACT-NGT on deck; rigged up German magnetometer.
	1830 5 June	Magnetometer test in pipe; lost 3-axis sensor at 1000 mbrf, but logged vertical field in hole.
	0700 6 June	Magnetometer on deck, minus lowermost 2 m of tool, which was left in hole.
	0900 6 June	"Wiper" pipe run to clear lost magnetometer piece.
7	1200 6 June	Schlumberger LSS-DIL-SFL-GR-CALI; required two runs because of computer problem on first run—excellent results.
8	0200 7 June	German magnetic susceptibility (with added weight); very good results.
9	1100 7 June	LDGO MCS + Japanese magnetometer; excellent data.
10	2100 7 June	Large-scale resistivity; excellent results.
11	0730 8 June	Schlumberger LDT-CNT-G-NGT including GPIT; excellent results.
12	1800 8 June	Offset to Hole 395C for sediment temperatures; ODP Von Herzen HPC; very good data.
	0015 9 June	Rigged up to trip pipe out of hole.
	0715 9 June	De-torqued reentry TV cable. Second pipe trip (packer in BHA)
	0700 10 June	Reentered.
13	1200 10 June	Packer; permeability tests at 396 and 536 mbsf.
	0945 11 June	Pull out of hole—time expired.
No time left to run:		
14		LDGO BHTV.
15		German temperature log.
16?		Flowmeter—not needed.
17?		Schlumberger DLL and possible repeat runs of logging tools that may have not performed as well as possible the first time.

prove measurement statistics but was not completed because of problems with the neutron source.

The next log on the schedule was the German three-axis magnetometer. During testing at 1000 mbrf, the three-axis sensor failed, leaving only the vertical-component gradiometer. The vertical-component log was completed successfully, and when the sonde returned to the surface we discovered that the lowermost weight had broken off, opening the lower electronics section and crushing the flask containing the three-axis sensor. The lost 2-m section remained in the hole.

The next scheduled run was the German susceptibility probe, which had the added advantage of being able to detect the presence of the lost section of the German magnetometer before hitting it. The sonde was too light to be run in the hole, so we fabricated a weight and ran a quick wiper trip (running the pipe to total depth and back to ensure that the missing piece was not lodged in the open hole). During the wiper trip, the fault in the Schlumberger sonic sonde was corrected.

Next, the DIL/LSS/SFL/GR/CALI sonde was run, recording two complete passes. No caliper information was recorded, and a software glitch during the first run prevented the recording of the full-waveforms, so the second pass with a different set of software was run to obtain the waveform data. The second log confirmed the measurements from the first pass, which included data on sonic velocity, natural gamma, and formation resistivity, as well as the recording of the sonic waveforms.

The German susceptibility log was run next, producing excellent results. The German tool also recorded electrical conductivity, which allowed the susceptibility log to be corrected for hole size; several spurious magnetic signatures were determined to be partly a result of washouts (enlarged sections of the well).

The next logging run consisted of the Japanese three-axis magnetometer/temperature probe, a self-contained digitally recorded device, combined with the multichannel full waveform sonic tool (MCS). Excellent sonic waveforms were recorded through much of the hole, although irregular hole size and borehole wall roughness caused problems in shallower sections. The Japanese device provided a measure of the magnitude of the horizontal components of the magnetic field, although the azimuth of the total-field vector could not be determined. Thus this run filled in some of the missing information from the German log. Temperatures recorded by the Japanese instrument confirmed the results of the earlier German log; however, because the data were recorded with the tool moving uphole, small-scale details of the temperature profile were lost.

We next ran large-scale resistivity experiment (LSR) to determine the resistivity of the formation several tens of meters away from the well bore. Because the results of this experiment in Hole 504B agreed well with the Schlumberger microresistivity log (SFL), we expected that the same would be true here. However, the Schlumberger log measures properties immediately adjacent to the borehole with a much greater vertical resolution than does the LSR; thus, the two data sets are complementary.

The Schlumberger lithodensity/neutron porosity/spectral gamma (LDT/CNT-G/NGT) combination was run next, with an additional probe (the general-purpose inclinometer tool (GPIT)) to monitor tool motion, azimuth and verticality of the borehole, and vector magnetic field. Two passes were run (one with the wireline heave compensator and one without) to measure its effectiveness in reducing wireline heave. Although the GPIT worked well, this test was only moderately useful because ship heave throughout the logging operations was <2 m.

At this point, we completed the first phase of logging operations and ran the pipe out of the hole. After the ship was offset

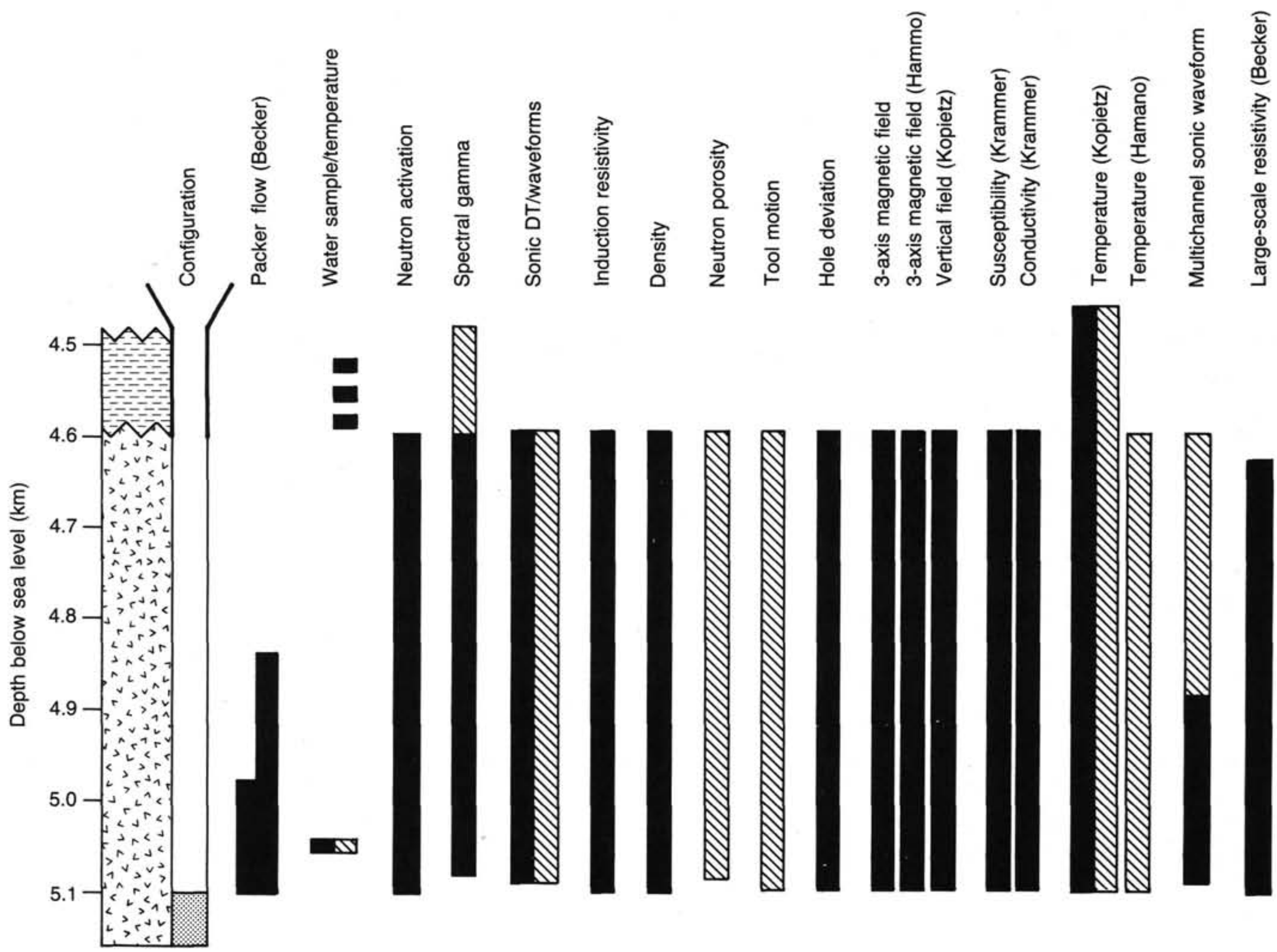

Figure 4. Operational summary of Leg 109 logging program in Hole 395A. The sediment/basement contact, the bottom of casing, and the current total depth of the hole are shown in kilometers below sea level. Estimates of the quality of the logging results are indicated by the line styles (solid line = good quality; patterned area = fair quality). The lines (solid and patterned) below the German temperature log (Kopietz) indicate the relative quality of the general profile and of the temperature gradient. The Japanese temperature log (Hamano) is graded "fair" because it was recorded with the tool moving uphole.

100 m northwest, Hole 395C was washed into sediments, and temperature measurements were obtained at 31, 58, and 84 mbsf to determine the heat flow at the site. These data, combined with the measured temperatures in Hole 395A, allowed the calculation of the flow rate of water down Hole 395A.

After completing the heat-flow measurements, we tripped pipe out of the hole and ran out the television-sonar system cable to remove residual torque and prevent snarling when next deployed on the drill pipe. This procedure was necessary because the camera had never been run below about 3400 mbrf. The second pipe trip was then initiated with a hydraulic packer for permeability and pore-pressure measurements. The television camera was run during reentry to confirm mud-line depth. Depth to the mud line was determined to be 4494 mbrf.

Two packer seats were obtained with the bit at 396 and 526 mbsf. Kuster mechanical pressure recorders were used to monitor downhole pressure, and water was pumped into the formation isolated by the packers to determine the permeability as a function of depth in the hole. Each Kuster tool recorded 6 hr of data, while a series of pulse and flow tests was made at each depth. Unfortunately, difficulties in retrieving the go-devil carrying the pressure recorders used up the rest of our time at the site; in fact, the second time the package was run it could not be retrieved, so it was carried to the surface during the final pipe trip.

At approximately 2000 hr on June 11, we left Site 395A, having obtained all but one of the planned logs. We spent a little over 9 days at the site. Slightly more than 1 day was spent on unforeseen operational contingencies, including reentry problems and detorquing the television-sonar system cable. In the 8 days devoted to science, we nearly completed the full 8-day logging program recommended for Hole 395A by the DMP.

Depth Conventions

Three different depth-counting systems were used during Leg 109 logging and experiments: (1) the carefully measured length of drill pipe, calibrated by the lengths required to touch mud line and the bottom of the hole; (2) a logging-cable depth counter run by Schlumberger for its logs; and (3) a separate logging-winch counter supplied by ODP for non-Schlumberger tools and experiments. The latter two counters gave inconsistent readings by about 20 m. It was essential to correct the results so that all Leg 109 depths are mutually consistent and are consistent with the lithology that was determined in coring Hole 395A during Leg 45.

The drill strings used during Legs 45, 78B, and 109 and the logging cables used during Legs 78B and 109 all probably stretched to different degrees. In a hole roughly 5 km deeper than rig floor, relative depths referred to rig floor may be inconsistent by as much as 20 m or more. Thus, instead of simply measuring depths from rig floor, it was more accurate to correct the log results to fixed points in the hole, such as seafloor, bottom of casing, bottom of the hole, and those boundaries within the formation that could be clearly seen in all the logs. On Leg 109, this was accomplished as follows:

During Leg 45 coring operations, the seafloor was determined by precision depth recorder (PDR) to be 4484 corrected mbsl. During Leg 109, the measurement of pipe length was consistent, as verified with the video reentry tool, by touching the bit to the seafloor before the second reentry; the pipe length on touching seafloor was 4494 mbrf, which is 11.1 m above sea level. During the first pipe trip, the bit was set on the bottom of the hole at 5100 mbrf, or 606 mbsf. (Hole 395A was originally drilled to 664 mbsf, but the lowermost 58 m has since been filled by cavings or has bridged over.) Given the known length of casing set in the hole, 112 m (extending through 93 m of sediment and the uppermost 19 m of basement), 494 m of open hole was available for logging during Leg 109.

The recorded depths of the logs could then be corrected to consistent depths below seafloor by calibrating the depths at which tools responded to the bottom of the casing and to particular features within the formation. In calibrating the Schlumberger counter, hole bottom was felt at a cable length of 5102–5104 mbrf, and casing was generally seen at about 4608 mbrf. The Schlumberger depths then had to be adjusted by about 2–4 m to be consistent with depths determined by drill pipe and PDR. In calibrating the ODP cable counter, the magnetic-susceptibility tool was set on bottom at 5121 mbrf, and casing was sensed by various tools at 4625–4630 mbrf. Thus, depths of the non-Schlumberger tools required a correction of about 21 m to be consistent with drill pipe. Depths of features used as reference points to correct cable counter depths are given in Table 3. For both counters and drill pipe, corrected depths are mutually consistent and relatively accurate to within 2–3 m.

TEMPERATURE MEASUREMENTS

Temperatures in Hole 395A and the surrounding sediments were measured several times during Leg 109 to describe as completely as possible the geothermal and hydrologic regime at the site. Detailed temperature measurements had been attempted during Leg 78B but were marred by instrumental failures and disturbances to the borehole fluids (Becker et al., 1984). Despite these problems, the Leg 78B data (Fig. 5) showed the following:

1. Ocean-bottom water was flowing down Hole 395A into the upper 200–300 m of basement, as indicated by nearly isothermal temperatures from mud line to about 300 mbsf.

Table 3. Reference points used to correct recorded log depths in Hole 395A.

Feature	Depth (mbsf)
Mud line	0
Bottom of casing	112
Magnetic reversal 1	261
Bottom of washout	428
Magnetic reversal 2	564

2. In the deepest section of basement, the gradient was probably conductive and consistent with the heat flow predicted for conductively cooling 7.3-m.y.-old crust.

The temperature-measurement program during Leg 109 was designed to test these conclusions and to determine accurately (1) the patterns of flow of ocean-bottom water down the hole and into the formation and (2) the equilibrium gradient in the deeper section of the hole. The rate of downhole flow could be determined, using the models of Becker et al. (1983a), from the difference of temperatures measured in the cased section and in the undisturbed sediments away from the hole. The equilibrium geothermal gradient in the sediments surrounding the hole is both the initial condition and a boundary condition for the mathematical treatment of the downhole flow, which must have started when Hole 395A was drilled in 1975. Downhole-flow rate must remain uniform with depth through the casing but is not necessarily uniform in the open hole, where some of the water flowing down the hole may exit radially into the formation. Continuous, high-precision temperature logging was planned, both to investigate the permeable zones into which the downhole flow is directed and to accurately measure the conductive gradient deep in the hole.

Operations

Ideally, all the necessary geothermal information on Hole 395A could have been obtained from a single, continuous, open-hole log of equilibrium temperatures immediately after reentry. However, the actual measurement program was more complicated because of operational considerations. Poor hole conditions had impaired drilling during Leg 45, and the hole had not been occupied since Leg 78B operations in 1981. Therefore, we considered it necessary to verify that the hole was open by running a bit to the bottom of the hole before allowing logging tools on a cable into the open hole. Critical undisturbed temperatures could be measured during this "clean-out" pipe run only by pausing and using ODP tools that protruded a short distance ahead of the bit.

Four different tools were used during the Leg 109 temperature measurements:

1. The ODP "Uyeda probe," which recorded every minute for 2 hr the resistance of a single thermistor encased in a 12.5-mm-diameter steel probe that extended 0.6 m ahead of the bit.
2. The ODP/Von Herzen APC heat-flow tool, programmed to monitor every 15 s for 3 or 4 hr the resistance of a single thermistor enclosed in the APC cutting shoe 0.3 m ahead of the bit.
3. The German BGR high-precision temperature-logging tool, described in detail later in this chapter.
4. The Japanese magnetometer, which incorporates a platinum resistor, as described in detail in the "Magnetometer Log" section (this chapter).

Five lowerings of these tools were made, in an order controlled partly by operational considerations:

1. Immediately after reentry, the pipe was run slowly and without circulation to 100.6 mbsf, near the bottom of the casing at 112 mbsf. With two joints of drill pipe made up in the derrick, a tandem combination of the ODP Uyeda probe plus APC heat-flow shoe was lowered on a wire rope to the bit, pausing first for a bottom-water calibration point at the mud line. When the probe had been seated in the bit, the pipe was slowly lowered, pausing at each joint for 10-min readings of undisturbed borehole temperatures at 100.6, 109.2, and 118.8 mbsf; then the probe was retrieved.

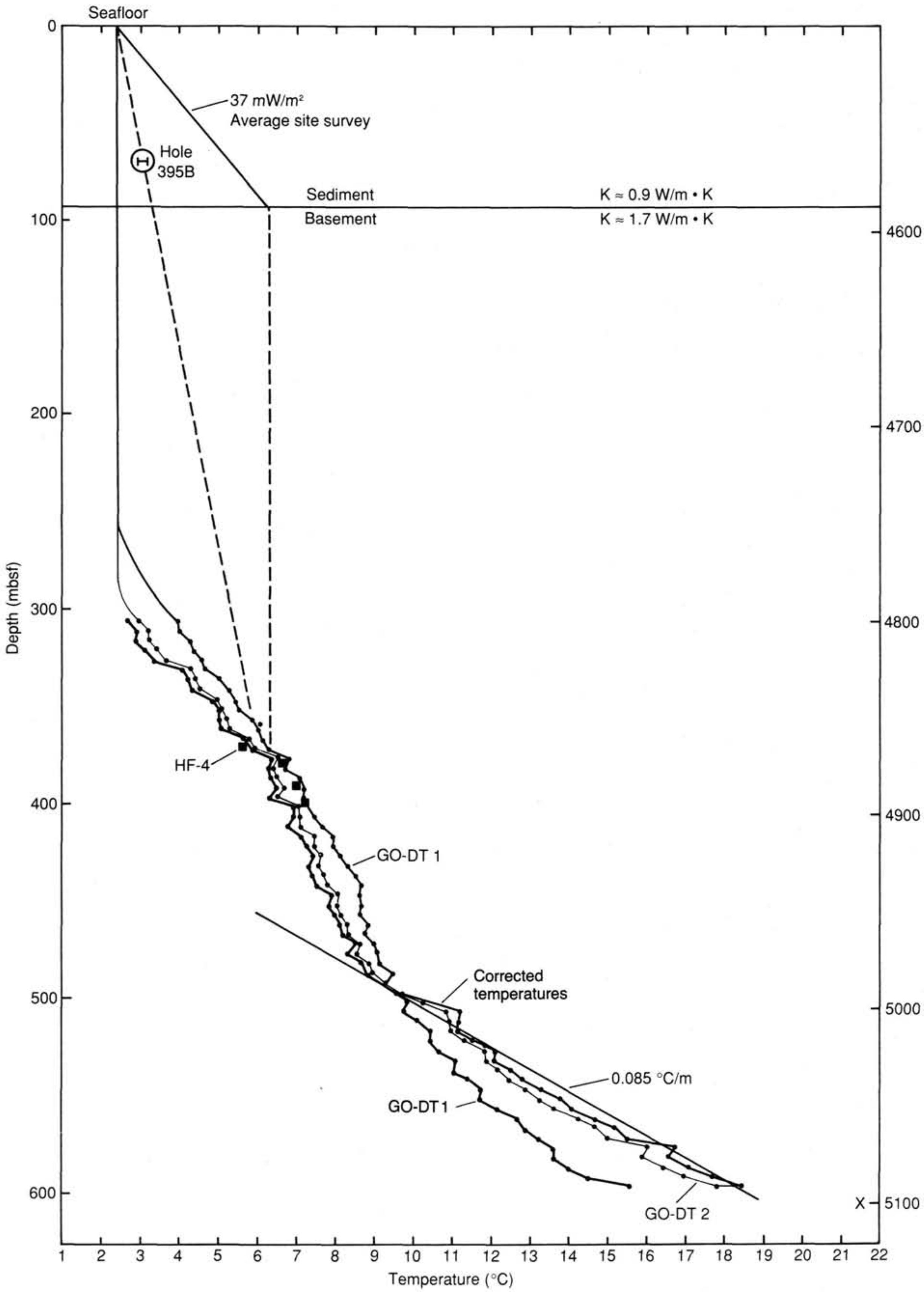

Figure 5. Temperatures measured in Hole 395A during Leg 78B. From Becker et al. (1984).

2. The pipe was then run slowly and without circulation or rotation extremely deep into the hole. Another lowering of the tandem ODP Uyeda plus APC tool, configured to take a sample of borehole fluids, was attempted. Unfortunately, neither temperature recorder worked properly, but a 45-mL sample was taken at 544 mbsf.

3. The pipe was then run to the bottom of the hole at 606 mbsf. The hole was found to be completely clean and to require no rotation or circulation to this point. Therefore, the disturbance to equilibrium borehole temperatures during this pipe run was minimal. The pipe was pulled slightly off bottom (to 592 mbsf), and the BGR temperature probe was used to obtain a high-precision temperature log within the pipe from mud line down to 582 mbsf.

4. After this log was made, the hole was conditioned for an extensive logging program by circulating for 30 min before pulling the pipe up into the casing. This was probably the only significant disturbance to borehole temperatures during the logging program. About 3 days later, the Japanese magnetometer was run, obtaining a continuous record of the borehole temperature while logging up the hole.

5. After spending 4 days logging Hole 395A, we pulled the pipe out of the hole and offset 110 m northwest, where Hole 395C was spudded solely to measure the background geothermal gradient in the sediments at Site 395. The ODP APC heat-flow tool was allowed to free-fall down the pipe and to latch into the bit. The bit was then slowly washed into the sediments, pausing three times to push without circulation 3–5 m into sediment, which we hoped would be undisturbed by the washing process. With excellent heave compensation, sediment temperatures were measured at depths of 31, 58, and 84 m into the sediments. (A similar heat-flow measurement in Hole 395B had been attempted with the Uyeda probe during Leg 78B, but the data were strongly disturbed by probe motion and circulation of drilling fluids or bottom water around the probe.)

Measurements with the ODP Probes and Calculation of Downhole-Flow Rate

The Uyeda probe and the APC heat-flow tool were combined for two lowerings in Hole 395C to ensure backup data collection in case of instrument failure. The Uyeda probe returned poor-quality data on both lowerings, and the APC tool worked for only the first, critical lowering near the bottom of the casing. An error in programming the APC tool was quickly corrected, and the tool worked well for sediment-temperature measurements in offset Hole 395C. Temperatures measured with the APC tool are shown in Figures 6 and 7.

Temperatures recorded in Hole 395C must be considerably processed to correct for the thermal disturbance, which affected the tool as it was washed and pushed into position for temperature measurements in the sediments. Unfortunately, the periods of these disturbances were somewhat longer than the times the probe was held in position for the measurements, and the theory normally applied to the HPC data (to correct for effectively instantaneous frictional heating on penetration) will be inadequate for correcting the data from Hole 395C. Nevertheless, it is apparent from Figure 7 that the measured temperatures are reasonably stable; the measurements suggest a temperature near the base of the casing (112 mbsf) on the order of 1°–1.5°C above bottom-water temperature. In contrast, Figures 6 and 8 show that temperatures in the borehole measured with BGR and ODP tools at the base of the casing are only about 0.03°–0.06°C, respectively, above bottom-water temperature.

This contrast confirms that ocean-bottom water is flowing down the hole, and a first-order estimate of the flow rate can be calculated with uncorrected data, following the quasi-steady-state model of Becker et al. (1983a). By balancing the total heat

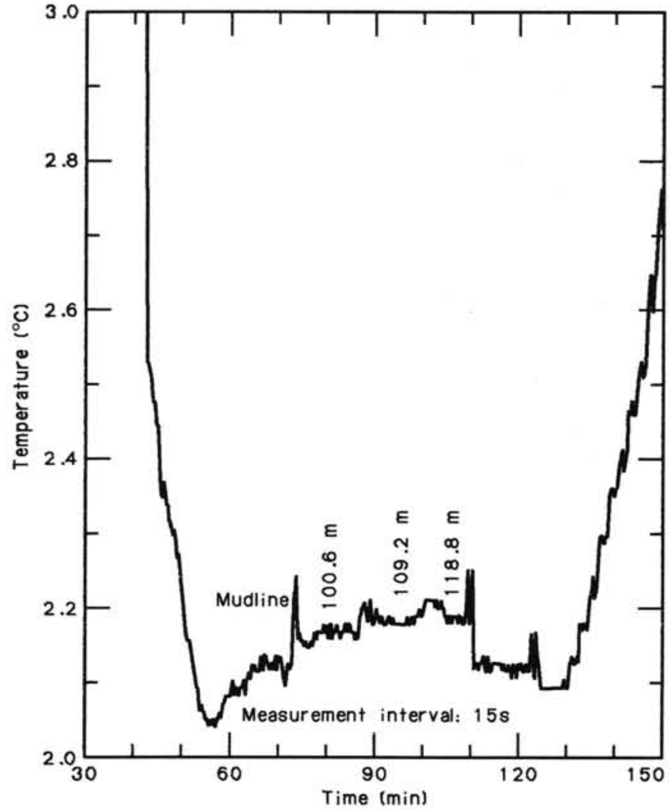

Figure 6. Temperatures measured on Leg 109 in the cased section of Hole 395A with the APC heat-flow tool.

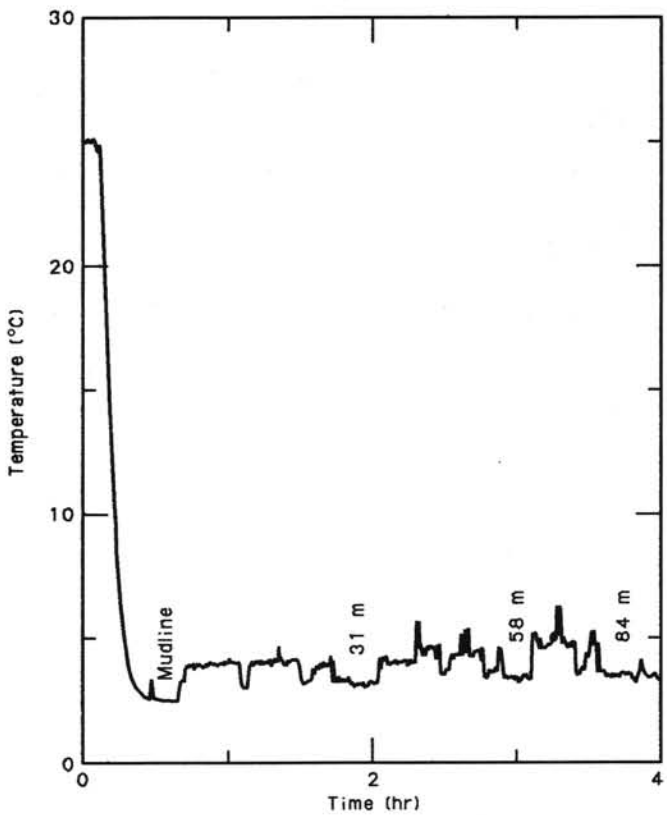

Figure 7. Temperatures measured on Leg 109 in the sediments of Hole 395C with the APC heat-flow tool.

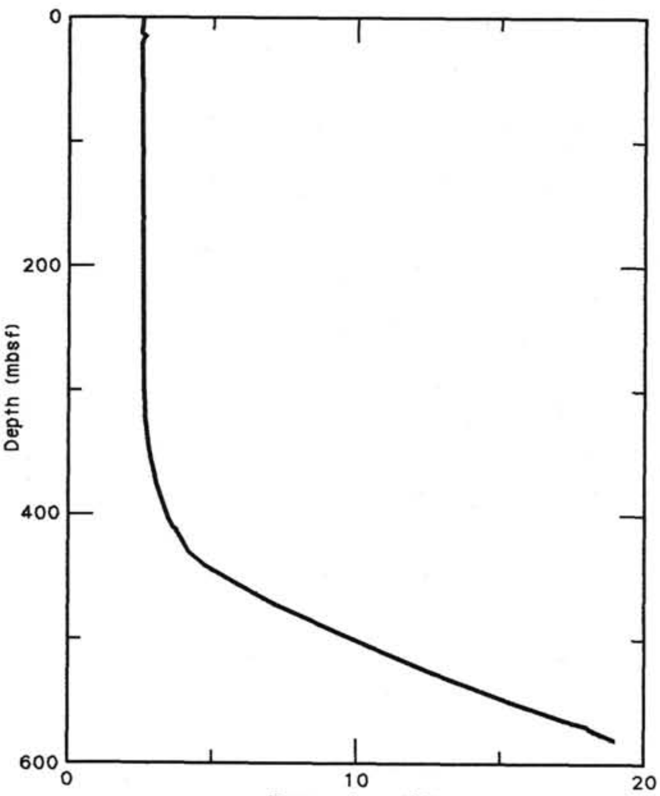

Figure 8. Temperature as plotted during downhole logging with the BGR temperature probe.

advected through the bottom of the casing with the downhole flow to the total heat radially conducted through the walls of the casing, an explicit expression can be derived for the linear flow rate, v:

$$v = 4hKI(t^*)[gh - T(h)]/pi^2a^2(pc)_wT(h),$$

where

h =	length of cased section	= 112 m
g =	geothermal gradient in sediment	= 0.014°C/m
gh =	sediment temperature at casing depth	= 1.53°C
$T(h)$ =	borehole temperature at casing depth	= 0.06°C
a =	radius of casing	= 14.9 cm
$(pc)_w$ =	volumetric heat capacity of fluid	= 1 cal/cm^3 s
K_e =	thermal conductivity of sediment	= 0.9 W/m K
t^* =	kt/a^2	= 3996
t =	time since flow started	= 3816 days
k =	thermal diffusivity of sediment	= 0.0027 cm^2/s,

and $I(t^*)$ is an integral derived by Jaeger (1942) in solving the problem of radial heat conduction about an isothermal circular cylinder. For $t^* = 3996$, $I(t^*) = 0.52$. Assuming parameter values as listed and using a preliminary estimate of the geothermal gradient (0.014°C/m based on uncorrected APC data) in the sediments, we obtain a first-order estimate of the flow rate of 18.7 m/hr, equivalent to a volume flux of about 1325 L/hr. This estimate will be refined in shore-based studies by first correcting the APC data to *in-situ* temperatures and then applying the more complete transient model of Becker et al. (1983a).

Measurements with the BGR Temperature Probe

The well-logging device for high-precision borehole temperature measurements developed at the Federal Institute for Geosciences and Natural Resources, Hannover, Federal Republic of Germany, basically consists of a probe with a 200-ohm platinum sensor of very low response time, a high-resolution digital multimeter for four-wire resistance measurement, and a desktop computer with plotter (Kopietz, 1984). Overall accuracy of the device is about 0.01°C. The resolution of the temperature measurements is about 0.001°C; the depth resolution (selectable depth intervals) ranges from 1 to 20 cm. The device has been modified for logging oceanic boreholes to withstand pressures of as much as 1 kbar and temperatures of as much as 320°C. (The temperature range depends mainly on the thermal property of the material used for sealing the probe and might be easily extended to temperatures on the order of 400°C.)

Before downhole logging, we performed an overall test calibration, including the logging winch and cable, which, owing to the length of the cable, yielded a correction of about 0.1°C to the calibration constant. To ensure a minimum disturbance of equilibrium temperatures, we planned to run the temperature measurements as soon as possible after reentering the hole. However, for safety reasons, we could not log temperatures until after a pipe run to clean the borehole, which had not been entered during the previous 5 yr. During this "clean-out" trip, the pipe was run down to the bottom slowly without circulation or rotation; the pipe was then left in the hole, and the first continuous temperature log was measured within the pipe, a procedure done for the first time, as far as we know. A second run was planned in the open hole at the end of the logging program to verify the measurements made in the pipe or to provide additional data for a possible extrapolation to equilibrium temperatures. However, no time was left for this second temperature log.

Hole 395A was logged in depth intervals of 2 cm at a downward speed of about 5 m/min. At the beginning and at the end of the logging run, test measurements on a reference resistor were made to confirm proper function of the electronic measurement device. The logging and measurement data are shown in Figure 8 and listed in Table 4.

An evaluation of the measurements applying a sliding regression for depth intervals of 5 m each time is shown on Plate 5 (in back pocket). Because the measurements were stored on tape only every 5 m, owing to a software error, this evaluation was made from the digitized plotter recording, which was generated during logging in intervals of 1 m (averages of measurement data). Apparently the temperature measurements were slightly affected by the heave motion of the temperature probe and possibly also that of the drill pipe.

From the top of the borehole (mud line) down to a depth of about 250 mbsf, a nearly isothermal temperature profile of very low variation was measured. As can be seen from the data listing (Table 4), temperatures of 2.53°C were measured at the top of the borehole and of 2.60°C at a depth of about 250 mbsf. From the temperature difference of these single measurements, 0.07°C, a mean temperature gradient of 0.28 mK/m across this section is obtained. A linear regression applied to this depth interval yielded a gradient and standard deviation of 0.25 ± 0.003 mK/m, thus verifying the precision of the measurements.

Below the isothermal section of borehole is an interval having a smoothly increasing temperature gradient to about 25 mK/m at a depth of about 430 mbsf. In the lower section of the hole, three temperature anomalies having a relatively sharp rise in the temperature gradient are recognizable: an increase of about 45 mK/m at depths of about 430, 475, and 530 mbsf. Between these anomalies, the gradients average about 100 and 120 mK/m, respectively, although they are slightly but significantly disturbed.

Table 4. Temperatures recorded in Hole 395A.[a]

Depth (mbsf)	Temperature (°C)	Depth (mbsf)	Temperature (°C)
5	2.531	300	2.666
10	2.526	305	2.687
15	2.540	310	2.678
20	2.623	315	2.695
25	2.568	320	2.688
30	2.536	325	2.699
35	2.536	330	2.714
40	2.538	335	2.721
45	2.549	340	2.748
50	2.535	345	2.778
55	2.543	350	2.835
60	2.536	355	2.857
65	2.535	360	2.891
70	2.540	365	2.949
75	2.551	370	2.996
80	2.556	375	3.057
85	2.570	380	3.119
90	2.548	385	3.186
95	2.560	390	3.241
100	2.551	395	3.319
105	2.562	400	3.406
110	2.560	405	3.492
115	2.557	410	3.584
120	2.565	415	3.705
125	2.564	420	3.850
130	2.603	425	3.976
135	2.560	430	4.096
140	2.557	435	4.227
145	2.572	440	4.413
150	2.566	445	4.672
155	2.561	450	5.019
160	2.591	455	5.417
165	2.574	460	5.754
170	2.565	465	6.142
175	2.573	470	6.386
180	2.588	475	6.818
185	2.583	480	7.330
190	2.585	485	7.890
195	2.581	490	8.392
200	2.590	495	8.780
205	2.587	500	9.313
210	2.591	505	9.706
215	2.590	510	10.377
220	2.591	515	10.721
225	2.603	520	11.242
230	2.599	525	11.750
235	2.599	530	12.263
240	2.596	535	12.812
245	2.608	540	13.488
250	2.607	545	14.108
255	2.604	550	14.781
260	2.642	555	15.278
265	2.625	560	15.921
270	2.653	565	16.435
275	2.646	570	17.189
280	2.647	575	17.813
285	2.651	580	18.347
290	2.649	585	18.848
295	2.652		

[a] Temperatures were recorded by the German BGR probe in depth intervals of 2 cm at a downward speed of about 5 m/min.

At the final depth of logging of 585 mbsf, a temperature of 18.9°C was measured.

Measurements with the Temperature Sensor Included in the Japanese Magnetometer

Information about the temperature-measuring capabilities of the Japanese magnetometer and about the logging run with that tool are included in the "Magnetometer Logs" section (this chapter). Plate 2 (in back pocket) shows the temperatures observed in Hole 395A, which were taken with the magnetometer, and shows the temperature gradient calculated from the temperature difference at 2-m intervals, logged upward with a speed of 2 m/min. Since the reproducibility and the resolution of the temperature measurement is <0.005°C, the calculated gradient shows stable variation. This is evident in the upper part of the hole (above 4800 mbrf), where the gradient is nearly zero.

The measured temperatures show a similar profile to that of the BGR temperature log made in the initial stage of the Leg 109 logging program in Hole 395A. This indicates that the logging operations between the BGR log and the Japanese magnetometer did not significantly affect the temperature distribution within the hole, in contrast to greater disturbances expected from drilling and circulation operations.

Preliminary Conclusions

In the upper and lower sections of Hole 395A, temperatures measured during Leg 109 are basically consistent with the results of previous temperature logs made in Hole 395A (Becker et al., 1984). However, an important difference appears in the intermediate section (250–430 mbsf). The nearly isothermal and largely undisturbed temperature gradient down to a depth of about 250 mbsf suggests a nearly constant rate of seawater flow down this section of borehole, which might exclude the possibility of a significant lateral flow of borehole water into the section. Below 250 mbsf, the continuous increase of the temperature gradient to a depth of about 430 mbsf may be due to an decrease of the downward flow, resulting from lateral flow into a formation of increasing permeability.

The observed anomalies in temperature gradient in the lower section probably indicate the main zones of outflow of seawater into the formation. The uppermost anomaly correlates with the extensive washout recorded on the caliper log during Leg 78B, which might be interrelated to a vigorous outflow of borehole water. According to this preliminary interpretation of Leg 109 temperature logging in Hole 395A, the zone of temperature disturbances by water movement reaches down to the lowermost borehole section. This is consistent with the results of the packer tests performed during Leg 109, which show that the lower section of the hole (396–606 mbsf) is quite permeable.

Predominantly conductive heat transfer is indicated only in two zones of the deeper section, where temperatures are less disturbed. The mean values of the temperature gradients of 100 and 120 mK/m obtained for these zones are about 25%–50% higher than the value extrapolated from the earlier measurements. The difference of about 20% in the temperature gradients for these zones might be caused by differences of the thermal conductivity of the formation. With a thermal conductivity of 1.8 W/m × °C, a heat flow of 180–216 mW/m^2 is indicated, which agrees well with the heat flow of 175–185 mW/m^2 predicted for a 7.3-m.y.-old, conductively cooling plate (Lister, 1977; Parsons and Sclater, 1977).

SCHLUMBERGER LOGS

During DSDP Leg 78B, a series of logs was run in the open section of Hole 395A from the casing shoe at 112 mbsf to a bridge at 606 mbsf (Hyndman, Salisbury, et al., 1984). These included resistivity, density, caliper, and sonic velocity logs run by a service company and a series of specialty logs provided by individual researchers; log quality was poor, however, and the results were ambiguous. During ODP Leg 109, Hole 395A was reoccupied to run a complete suite of state-of-the-art logging tools in the open hole.

The experimental program was developed both to improve the quality of the logs already run in the hole and to collect additional log measurements not available at the time of Leg 78B. Log measurements obtained by Schlumberger include resistivity, sonic velocity, formation density, porosity, and natural gamma activity, all being logs run during Leg 78B but which either failed or gave results of uncertain quality.

In addition, a set of geochemical measurements was obtained using two new techniques. One measures the spectral content of natural radiation to determine the concentrations of potassium, uranium, and thorium in the formation. The other uses a neutron-activation technique to determine the concentrations of the primary rock-forming elements, including Si, Ca, Fe, Al, Mn, S, H, and Cl. These new logs were developed for use in sediments and were run here for the first time in igneous rocks.

Measurements

The aforementioned logs were collected during three lowerings of the Schlumberger combination tools. The first lowering was the DIL/LSS/SFL/GR/CALI combination, which measures formation resistivity, sonic velocity, natural radiation (for depth correlation to other logs), and hole size. Hole size was not measured because of a tool malfunction, but, fortunately, it had been measured accurately during Leg 78B and, thus, did not need repeated measurement. The first deployment of this combination was unsuccessful, but the second attempt succeeded in recording excellent data from the casing shoe at 112 mbsf to just above the bridge at 606 mbsf. A second pass was run to record sonic waveforms in the open hole.

The second lowering was the geochemical combination GST/ACT/NGT tool, which allows determination of the concentrations of U and Th in ppm, K in weight percent, and the relative concentrations of Si, Ca, Fe, Al, Mn, S, Cl, and H. Absolute concentrations can be determined if careful core calibrations are made. This log is run very slowly (about 100 m/hr); for best results at least two passes must be made in the hole. We ran one complete pass, but before the second pass was under way, the neutron source began behaving erratically, so we terminated the log run.

The final Schlumberger lowering was the LDT/CNT-G/NGT combination, which measures formation density and porosity and provides an additional pass of the K/U/Th log. During this lowering, an extra device was deployed to monitor tool motion to study the efficiency of the wireline heave compensator. This device (designated GPIT) also measures hole azimuth, deviation from vertical, and the three components of the local magnetic field (with respect to tool position). Two complete passes were obtained at different logging speeds, and a third pass with the heave compensator turned off was run over a short section near the top of the logged interval.

Results

Plate 1 (in back pocket) presents the primary log curves. The primary petrophysical data, including porosity, density, and the calculated concentrations of U, Th, and K are shown on the left; in the middle are the velocity and resistivity curves, along with the large-scale resistivity log discussed later in this section. The raw count rates measured by the geochemical tool suite are on the right. The GPIT measurements are not presented in the plates because they are primarily recorded as an engineering exercise to test the performance of the heave compensator. Figure 9 is a summary plot showing the relationship between DSDP Leg 45 core and ODP Leg 109 log data.

These logs were recorded using the Schlumberger depth encoder. Depths were referenced to the bottom of each tool and zeroed at the drilling stool 11.1 m above sea level. Because the sensors are spaced at intervals along the tool string, the deepest measurement recorded by each sensor depends on its position. The logs were run from close to total depth (TD) until the entire tool string was above 104 mbsf. Each logging run includes a natural gamma curve for depth correlation. The position of the casing shoe was detected by most of the log curves at 112 mbsf. The Schlumberger log curves can be correlated to within 1 m throughout the hole. A 5-m difference in the apparent depth of casing was observed during the GST logging run; because this difference is not observed for other features, we made no additional correction.

Log Descriptions

Standard gamma (SGR) measures natural radiation as a function of depth, for depth correlation between logging runs, in API units. For comparison, typical values in air are 10–20 units; in shales the values can be >100. A low value indicates a very low percentage of radioactive elements.

Resistivity is the resistivity of the formation and is generally a function of porosity. Three measurements obtained by the DIL sonde (ILD (deep induction), ILM (medium induction), and SFLU (spherically focused laterolog)) are displayed in Ω-meters. In general, the SFL is a higher quality log in resistive formations (greater than a few hundred Ω-meters). Enlarged sections of the hole cause low readings.

The Vp (compressional-wave velocity), NPHI (porosity as a ratio), and RHOB (bulk density in g/cm^3) logs plot to the right in hard competent material and to the left in soft, washed-out material. The porosity in basalts generally reads somewhat high (e.g., Broglia and Moos, in prep.), showing an approximate 20% mean value for the log. The density readings are generally between 2.6 and 2.8 g/cm^3 in "hard" sections where the resistivity is >100 Ω-m. Vp in core samples is about 6 km/s (Melson, Rabinowitz, et al., 1978); in the hole it is typically between 3 and 6 km/s except where spurious low values are measured in washed-out zones.

K (weight percent), U, and Th (ppm) are from the NGT log. The concentration of all three is extremely low, confirming the low gamma-ray readings. Kicks in the concentrations probably correspond to zones of fracture infilling.

CSIG, the cross section of thermal neutron capture, is sensitive to Cl, H, and B, primarily in the borehole fluid, and to small amounts of high-capture elements in the cross section, such as Gd. CSUL is the count rate for S; in this hole it should be sensitive to massive sulfides. CFE is the Fe count rate. CCHL (Cl) and CHY (H) are affected primarily by the borehole fluid. In this hole they are excellent indicators of washouts. ASST is the Al count rate; CCA and CSI are the count rates for Ca and Si, respectively. All these curves are strongly affected by hole size. Comparison of these curves to the caliper log run during Leg 78B emphasizes this effect.

Figure 10 shows the results of the GPIT log measurements, which give environmental information about tool motion and position, as well as the x, y, and z components of the magnetic field (measured with respect to the tool). DEVI is the tilt of the borehole with respect to vertical. AZ is the vertical acceleration of the tool. Variations from $g \cong 9.8$ are due to ship heave and stick-slip motion of the tool in the borehole. The three components of the Earth's magnetic field are determined relative to the orientation of the tool. Unfortunately, the tool does not have a fixed reference frame, so the azimuth of the magnetic field vector cannot be determined uniquely. However, the magnitudes of the horizontal (FH) and vertical (FZ) field components can be determined. FINC is the inclination of the magnetic field vector, and FNOR is the intensity of the magnetic field. Note sharp changes in magnetic field at 261 and 564 mbsf, corresponding to magnetic reversals. These points were used to tie depth with the magnetometer runs recorded by the ODP depth counter.

Discussion

Figure 11 is a composite of the primary log measurements obtained during Leg 78B. Included are hole size (caliper), formation density, resistivity, and sonic velocity. Of these logs, only

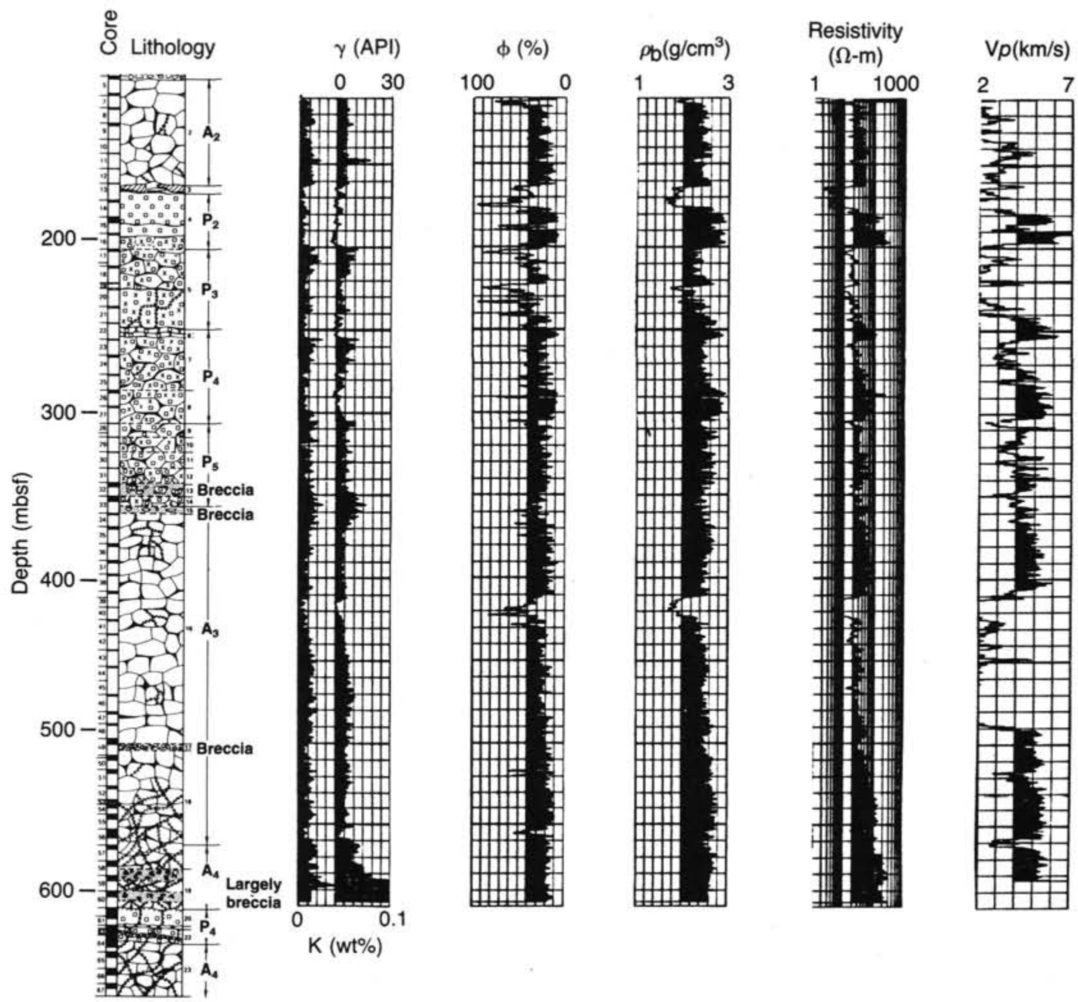

Figure 9. Composite log of Hole 395A, showing petrophysical information, from left to right: concentration of potassium (K) in weight percent; natural gamma radiation; porosity; density; resistivity; and sonic velocity.

the caliper results were of consistently high quality. Velocities in the uppermost 400 m are <2.0 km/s, unreasonably low even for the highly porous basalts of layer 2A. Densities are quite variable, not surprising because the great irregularity of the hole degrades the quality of the density log, which depends on good coupling between the measurement pad (which is pressed to the borehole wall) and the formation. However, average values are not unreasonable. Resistivities are between 20 and 60 Ω-m in the uppermost section and increase to >200 Ω-m in certain intervals. Natural gamma is <10 API units. Of primary interest for development of a preliminary log interpretation is the caliper log, which reveals that the hole is washed out throughout almost the entire section. Several large holes occur at 175–185, 200–250, and 410–425 mbsf, and innumerable smaller washouts are present. Below 425 mbsf, the hole is more nearly to gauge.

The measurements obtained during Leg 109 are also strongly affected by hole size (see Plates 1 and 2 (in back pocket) and Fig. 9). This is true not only for such indicators as H and Cl concentration but also for porosity, density, and in extreme cases for resistivity (for instance, at 414–429 and 164–180 mbsf). Washouts also reduce the amplitude of the refracted sonic wave, causing erroneous picking and spurious velocity determinations.

Strong cyclicity is evident in many of these log measurements. Boundaries occur at 179, 204, 229, 259, 359, and 414 mbsf, each having a steplike increase; the intervals between these levels show steady CSIG decreases. Similar boundaries are seen on the other logs. For instance, resistivity decreases at each of these boundaries and increases below them, as does density and to a lesser degree sonic velocity. These variations were interpreted during Leg 45 to indicate lithologic variations (Mathews et al., 1984). Interestingly, however, CHY and CCHL also display a similar behavior, and the caliper log shows some of the same trends. Clearly, more careful analysis must be made before these variations can be ascribed to lithologic differences.

Crossplots of the different measurements provide a primary log-analysis tool. Figure 12 shows porosity as a function of bulk density for the log data. Shown also is a linear least-squares fit to the shipboard physical properties measured during DSDP Leg 45 (Melson, Rabinowitz, et al., 1978). An ad-hoc correction was applied to the log data by subtracting 8 percentage points from the porosities, following the example of Broglia and Moos (in prep.). After this correction, low-porosity data lie on the best-fit line, but at higher porosities the data plot somewhat below the line. This suggests that the simple ad-hoc correction may not be adequate for data from this hole.

Figure 13 shows the logged compressional velocity vs. density. The linear least-squares fit to laboratory data is also shown (Melson, Rabinowitz, et al., 1978). Here the trend in logging data suggests that log velocities are less sensitive to density variations than the laboratory data suggest. This agrees with the results of Broglia and Moos (in prep.) and implies that *in-situ*

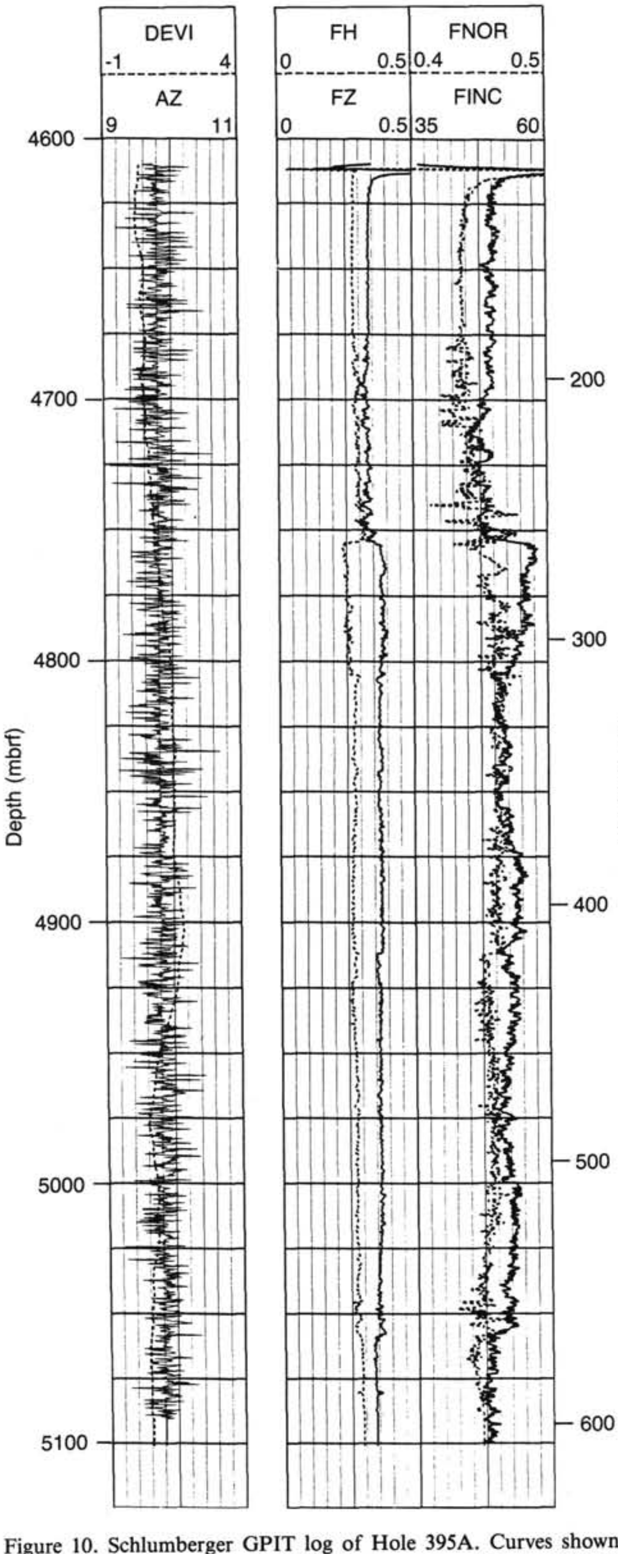

Figure 10. Schlumberger GPIT log of Hole 395A. Curves shown are hole deviation from vertical (DEVI) in degrees; vertical acceleration of the logging tool (AZ) in m/s^2, including the Earth's gravitational field, ship heave, and stick-slip tool motion; the horizontal (FH) and vertical (FZ) vector components of the Earth's magnetic field in Gauss; the computed magnitude of the field vector (FNOR) in Gauss; and the inclination of the field (FINC) in degrees. Depths below seafloor were computed by subtracting 4496 from depth below rig floor. The effect of casing at 112 mbsf can be seen in the magnetometer results above about 125 mbsf.

density variations are due in part to variation in large-scale (fracture) porosity.

Summary

These logs are consistent with similar results from Leg 78B; however, sonic velocity is more reasonable and resistivity is somewhat lower. Comparison of the density and porosity data must await further processing. Strong cyclicity appears in these logs; however, this may be due partly to cyclic variations in hole size.

Competent units having velocity >5 km/s, resistivity >100 Ω-m, and density >2.6 g/cm^3 occur in the intervals of 184–189, 194–199, 254–259, 289–294, and 384–394 mbsf, and in the lowermost 75 m of the hole. Elsewhere in the well, velocities range from 3.5 to 4.5 km/s, densities are highly variable, and resistivities range from 20 to 100 Ω-m. These values are typical of the uppermost few hundred meters of oceanic layer 2 (see, for instance the results of Hole 504B studies of Anderson, Honnorez, Becker, et al. (1985)).

The geochemical logs are unique, both in that they were not available before this leg and that they have never been run in hard-rock environments. The concentrations of uranium, potassium, and thorium are very low, consistent with the low natural radiation and with our expectations of these basaltic rocks. The remaining curves are quite sensitive to hole size and must be corrected before they can be meaningfully interpreted.

The hole inclination is everywhere <2°, which is remarkable considering the nature of the shallow oceanic crust. The magnetometer results indicate a reversal at 261 mbsf and another at 564 mbsf. These depths were used to constrain the depth measurements during the other two magnetometer-logging runs.

Conclusions

One of the primary objectives of basement logging at Hole 395A was to determine the seismic properties, porosity, and density of the uppermost few hundred meters of oceanic layer 2. According to these preliminary results, these properties are variable on scales of a few tens of meters. No strong evidence of a well-developed layer 2A exists at this site, although velocities characteristic of this layer occur at scattered intervals. More likely, the uppermost few hundred meters of basement is a highly heterogeneous mixture of pillows, partly cemented pillows, and competent units.

MULTICHANNEL SONIC LOGGING

The multichannel sonic (MCS) log was run in Hole 395A to measure the elastic properties of the basement section. This log complements the Schlumberger sonic log by providing a better measurement of sonic compressional and shear velocity. During the logging run, 12 sonic waveforms are recorded at each source depth. In addition to showing velocities, analysis of these waveforms provides measurements of the frequency and energy of the propagating waves.

The MCS log has been run in several wells on land, and a prototype version was run in DSDP Hole 504B during Leg 92 (Moos et al., 1986). Since that time, data were obtained in DSDP Hole 418A during ODP Leg 102 (Moos, in prep.) and at a series of sediment sites during ODP Leg 103.

Description and Operation

A schematic drawing of the MCS sonde is shown in Figure 14. A single acoustic source is positioned uphole from an array of 12 receivers spaced 15 cm apart. The distance between the source and the first receiver can be varied by inserting a decoupling spacer between the source and receiver sections. During operations at Hole 395A, we used a 3-m source-to-first-receiver gap.

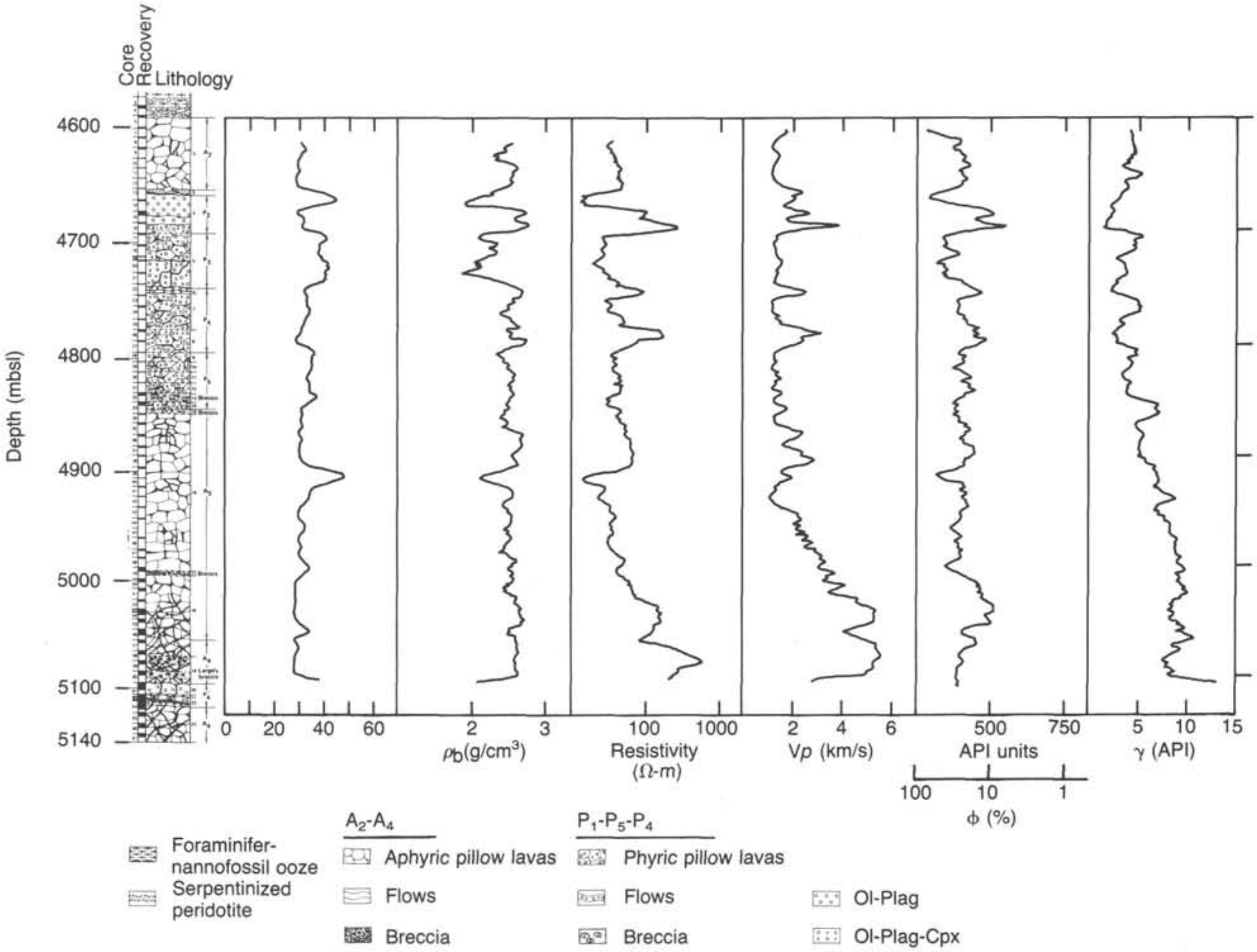

Figure 11. Logging results, Leg 78B, showing, from left to right, the following logs: caliper, density, resistivity, sonic velocity, porosity, and natural gamma radiation. After Mathews et al. (1984).

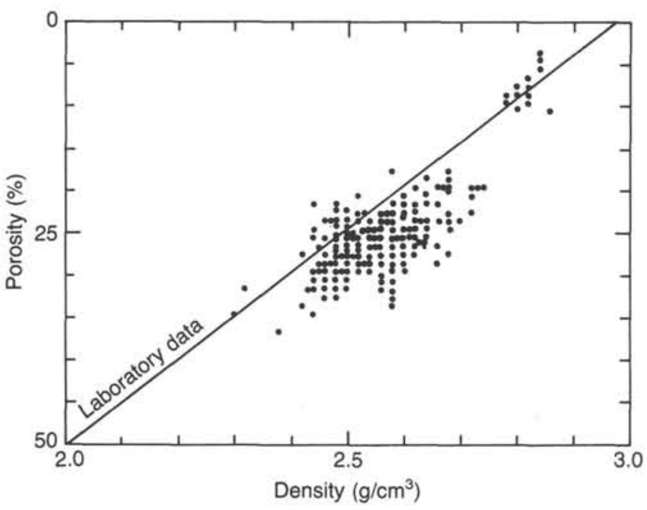

Figure 12. Crossplot of porosity vs. density values from Hole 395A. Porosity was corrected by subtracting 8 percentage points. Shown also is the best-fit line to shipboard laboratory measurements of porosity and density (Melson, Rabinowitz, et al., 1979).

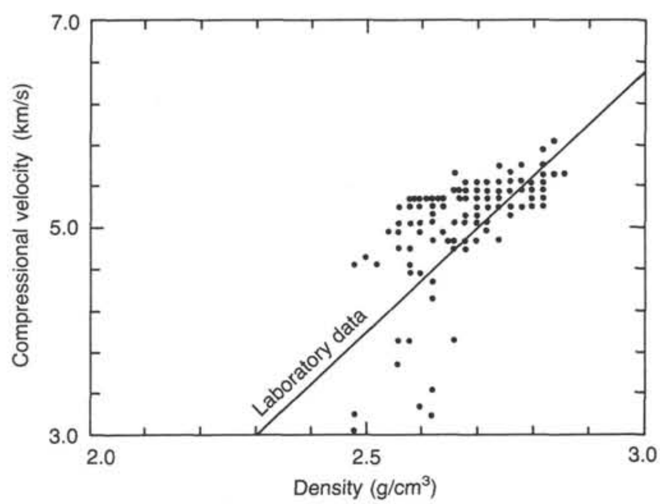

Figure 13. Crossplot of velocity vs. density values from Hole 395A, with the best-fit line to shipboard laboratory measurements (Melson, Rabinowitz, et al., 1979).

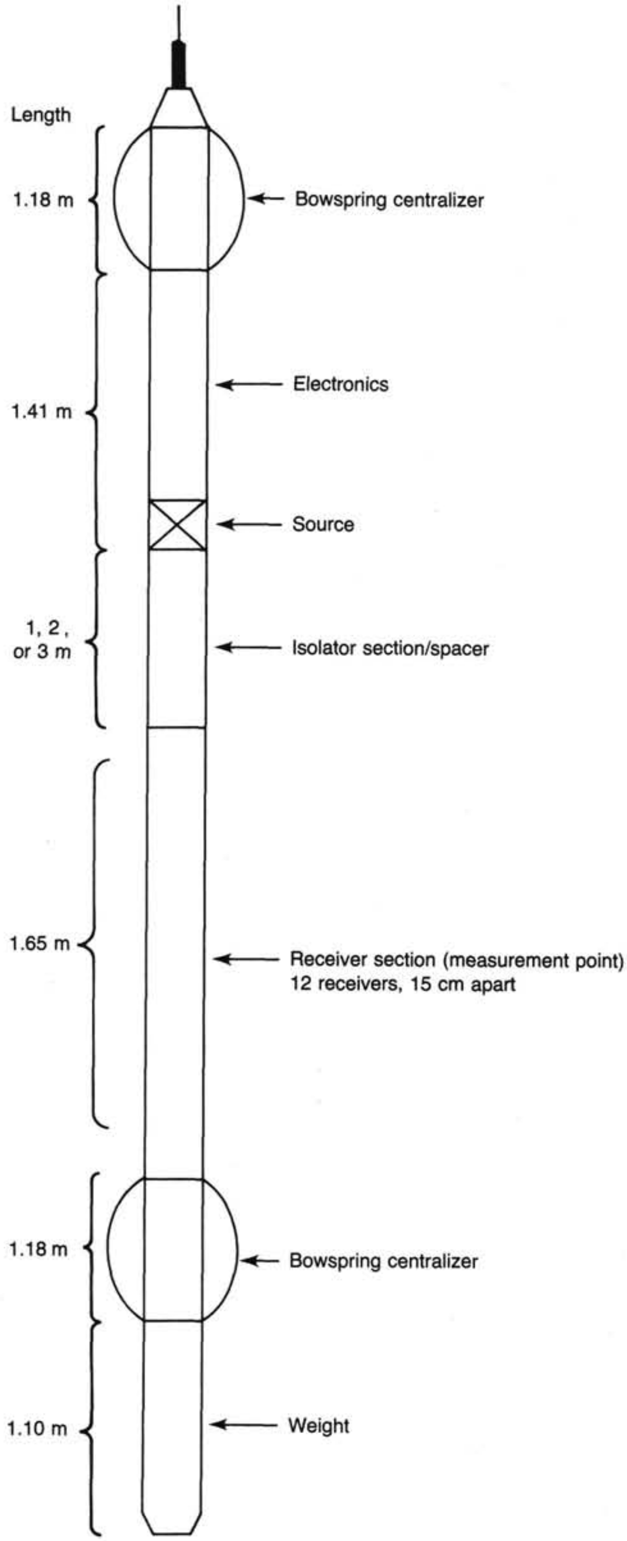

Figure 14. Schematic drawing of the MCS logging sonde.

During operations, the tool was raised or lowered in the hole at a constant rate, and a suite of 12 waveforms was recorded at fixed depth intervals. To produce the 12-receiver suite, the source was fired 12 times and the receivers were polled in order. The amplifier gain and receiver number were controlled from the surface.

The MCS log was run in the hole after the German magnetic-susceptibility tool (Table 2). To run the Japanese magnetometer/temperature probe without sacrificing logging time, a crossover was built, and the Japanese probe was hung below the MCS sonde in place of the usual sinker-bar. This prevented the recording of data from the lowermost 7 m of open hole. The logging tool was run in the hole to just above the bottom of the pipe, and a downgoing log was recorded that had a high borehole gain. The rate of descent was approximately 5 m/min, and more than 2000 waveforms were recorded over the open-hole interval. Once the downgoing log was completed, we had to wait for approximately half an hour for the clock in the magnetometer to initiate its recording cycle. The upgoing log was started shortly after the magnetometer was actuated, and the uphole log was recorded at a lower borehole gain. To take advantage of the 5-hr recorder period of the Japanese tool, the uphole log was run at approximately 2 m/min, resulting in an open-hole log from 595 to 112 mbsf (the casing depth). The logging started above the bottom of the hole to prevent the probes from becoming entangled with a missing section of the German three-axis magnetometer. During the upgoing logging, more than 5000 waveform suites were recorded; 10 suites were recorded for each meter of open hole.

The waveform data were transmitted to the surface in analog form, and digitized at 2-ms intervals by the LDGO MASSCOMP logging computer. The digitized data were stored on magnetic tape. After the log was complete, the data were played back and analyzed to determine compressional and shear velocities and the energy and frequency of the refracted arrivals.

Data

Figure 15 shows a sample suite of waveforms recorded in a hole drilled through granodiorite. Each received signal is displayed at an offset corresponding to the receiver position. The principal wave-mode arrivals are illustrated in this figure. The first arrival is a compressional head wave, which propagates along the borehole wall, arriving at the receivers at a time linearly related to their distance from the source. The traveltime between successive receivers divided by the distance between them is defined as the "slowness" of the propagating pulse. Its inverse is the velocity. The next arrival is a shear headwave. This is followed by a series of normal modes, which give the shear arrival a ringed appearance. The first normal mode, or pseudo-Rayleigh wave, travels at just below the shear velocity of the formation. The last prominent arrival is the Stoneley wave, an interface wave that travels at just below the fluid compressional-wave velocity. The Stoneley wave is a low-frequency wave that propagates efficiently in smooth boreholes having diameters only slightly greater than the diameter of the logging sonde. In washed-out or enlarged sections, the Stoneley wave does not propagate; if the hole is large enough, a true high-frequency fluid arrival can be seen.

Figure 16 shows the waveform recorded at the fourth receiver, which is plotted as a function of depth below seafloor. These are also displayed in Plate 1 (in back pocket). Shown also is formation resistivity from the Schlumberger SFL log. The main feature of this data is the prominent low-frequency, high-amplitude oscillation that interferes with the recorded signal throughout the hole. The source of this energy is uncertain, as there is no indication that energy propagates along the tool itself when the tool is on the surface. This interference complicates the analysis of the elastic characteristics of the formation. Fortunately, significant parts of the hole are not seriously affected. Strong formation arrivals can be seen at several depths in the hole. Two 5–10-m-thick intervals at 180–200 mbsf and a short section at about 260 mbsf, the intervals at 285–300 mbsf, 360–410 mbsf, and the lowermost 120 m of the hole all show

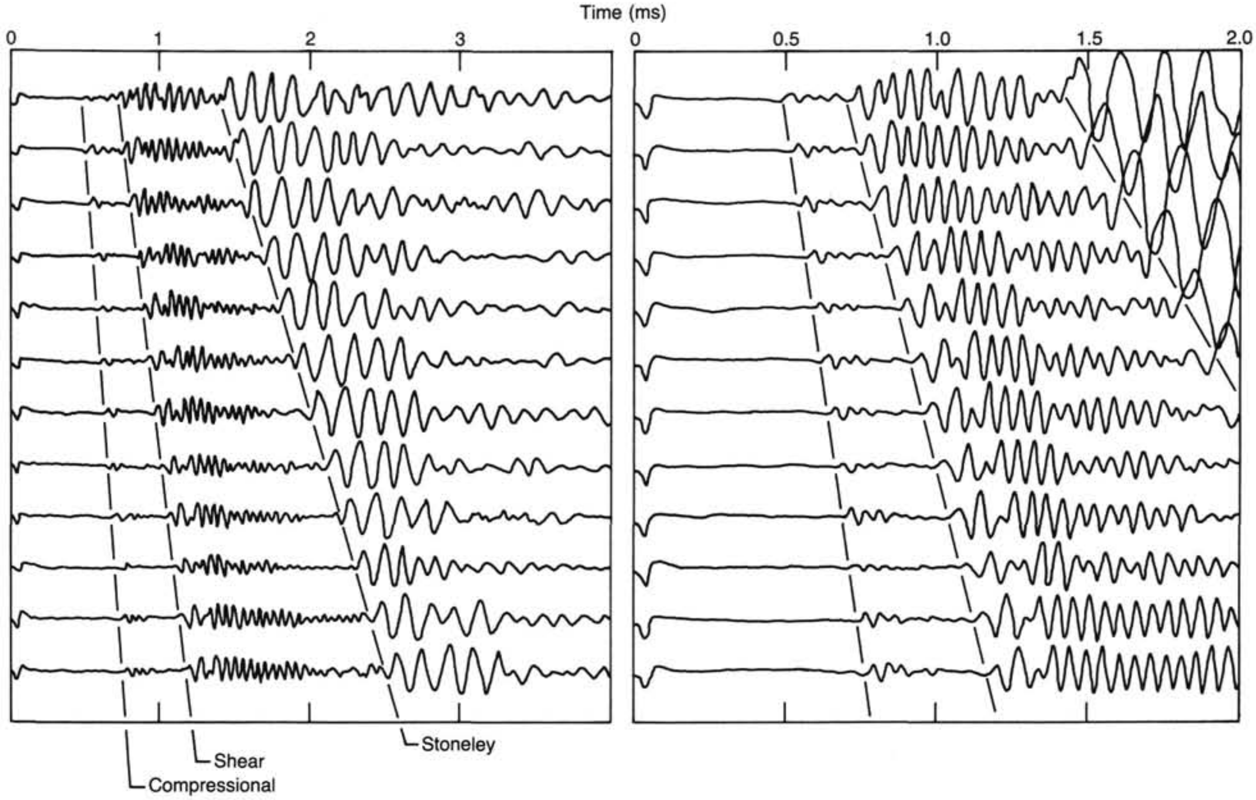

Figure 15. Sample waveform suite from unfractured granodiorite, showing the expected arrivals in hard rock.

high-amplitude, high-frequency compressional arrivals. In general, intervals with high resistivities also have higher recorded amplitudes; conversely, low-resistivity or washed-out intervals return very little coherent energy. These variations can also be correlated with characteristic features in the recovered cores (Melson, Rabinowitz, et al., 1978) and in the other logs (Plates 1 and 2, in back pocket). For instance, in the lowermost section, cracks in the core were surrounded with alteration halos; elsewhere in the hole, this alteration style is also associated with zones of high amplitude refracted arrivals. Additionally, the interval just below 280 mbsf has significant amounts of breccia. Further interpretation must await more careful depth correlation and data analysis.

To further emphasize the variability in the recorded waveforms, Figure 17 shows suites of waveforms recorded during the downgoing logging run at 365, 475, 516, and 555 mbsf, respectively.

At 365 mbsf, the direct arrivals are obscured by interfering energy. However, the presence of higher frequencies in the data suggests that some information may be recoverable from these waveforms. At 475 mbsf, a strong compressional arrival is present, but little shear energy is seen. At 516 mbsf, all the classic wave modes are present. At 555 mbsf, the data are clipped; however, the lower amplitude data recorded during the upgoing logging run can be used to calculate velocities and propagation characteristics.

Data Analysis

Velocities are calculated from the recorded waveforms, using a modified semblance technique. The semblance is computed by summing the cross correlation of each possible waveform pair (suitably time shifted) and then normalizing this by the sum of the autocorrelations of the data in each window. This calculation produces a number that varies between 0 and 1, depending on the degree of correlatability of the waveforms within the windows. By changing the path through the data along which the window is run, different wave-mode arrivals can be isolated. The slowness for a given arrival is the slope of this trajectory that gives the highest semblance. The velocity of the windowed mode is then simply the inverse of the slowness.

Figure 18 shows the results of preliminary semblance calculations on data from the lowermost 100 m of Hole 395A. Compressional and shear velocity, the semblance result using the best-fit velocity, the velocity ratio, and the mean semblance are plotted as a function of depth. Velocity calculations that result in semblance values <0.3 are disallowed. This lowermost section of the hole (from 495 to 595 mbsf) has uniformly high velocities and high semblance. Compressional velocity varies between 5.0 and 6.0 km/s, and shear velocity varies between 3.0 and 3.5 km/s, yielding V_p/V_s ratios of 1.7–1.8. Low semblance at 555 mbsf indicates a fractured or washed-out zone. Above 495 mbsf, shear semblance drops below 0.3 and compressional semblance begins to track the interfering signal. Examination of the waveforms in Figure 16 reveals that this is the depth at which the direct arrivals begin to be obscured by noise.

These compressional velocities are similar to those determined by the Schlumberger LSS sonde. Furthermore, the fact that in the lowermost part of the hole the velocities are close to those measured on laboratory samples (Schreiber and Rabinowitz, 1978) suggests that the *in-situ* material has very low porosity and that any fractures are probably sealed. The low amplitudes elsewhere in the hole suggest that this is not true for the entire depth section.

Conclusions

Over 7000 full waveform suites were recorded in Hole 395A using the MCS logging sonde. Preliminary analysis of the waveforms suggests that their amplitude and frequency content may

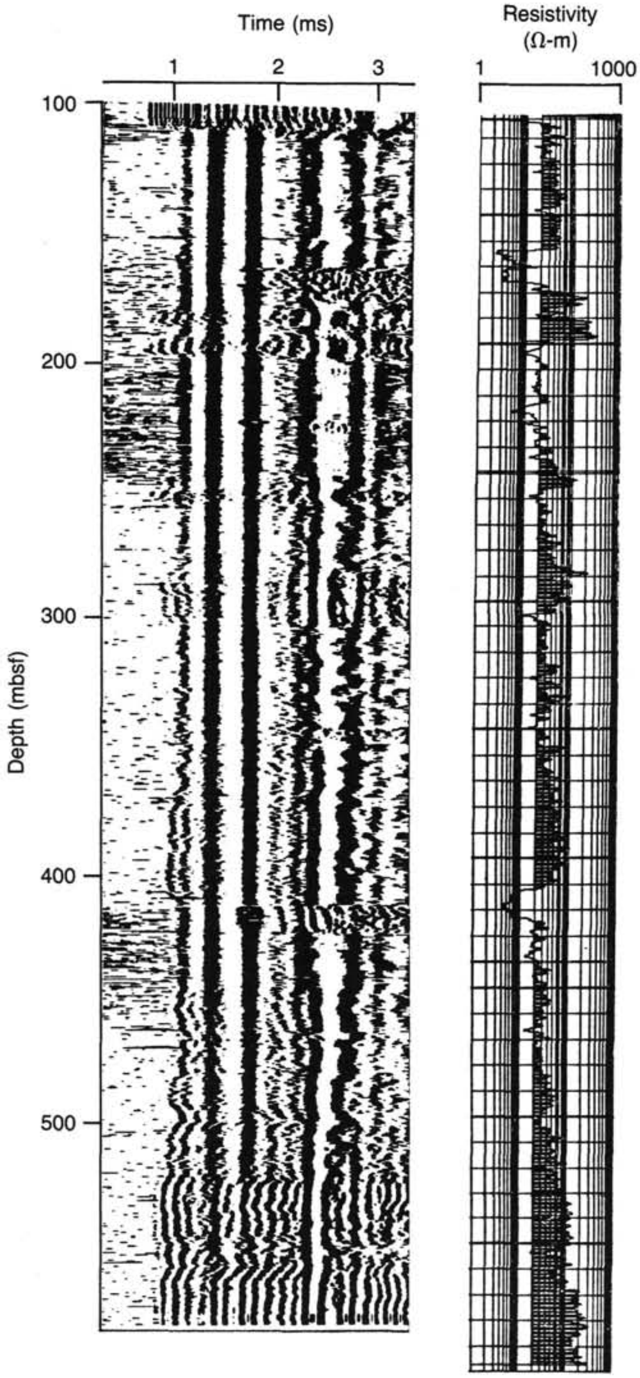

Figure 16. Waveform recorded at the fourth receiver, which is plotted as a function of depth. Casing is at 112 mbsf (note high-frequency arrivals). Shown also is resistivity measured by the Schlumberger SFL.

be related to lithology. Where velocities were calculated from the recorded waveforms, compressional velocities are close to the laboratory measurements, and shear velocities are high, suggesting that the lowermost 100 m of the hole (except the short section at 555 mbsf) has low porosity and that any fractures are well sealed. Analysis of data from the rest of the hole, where these conditions certainly do not exist, has not been completed.

MAGNETOMETER LOGS

Downhole measurements of the magnetic field within ODP and DSDP holes can be a useful counterpart to the paleomag-

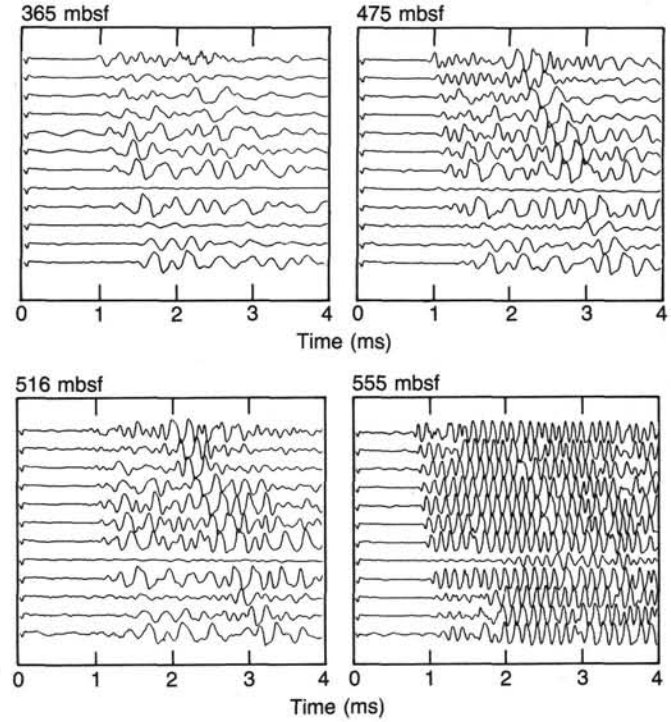

Figure 17. Waveform suite recorded at 365, 475, 516, and 555 mbsf, showing variation in amplitudes caused by lithologic variations within Hole 395A.

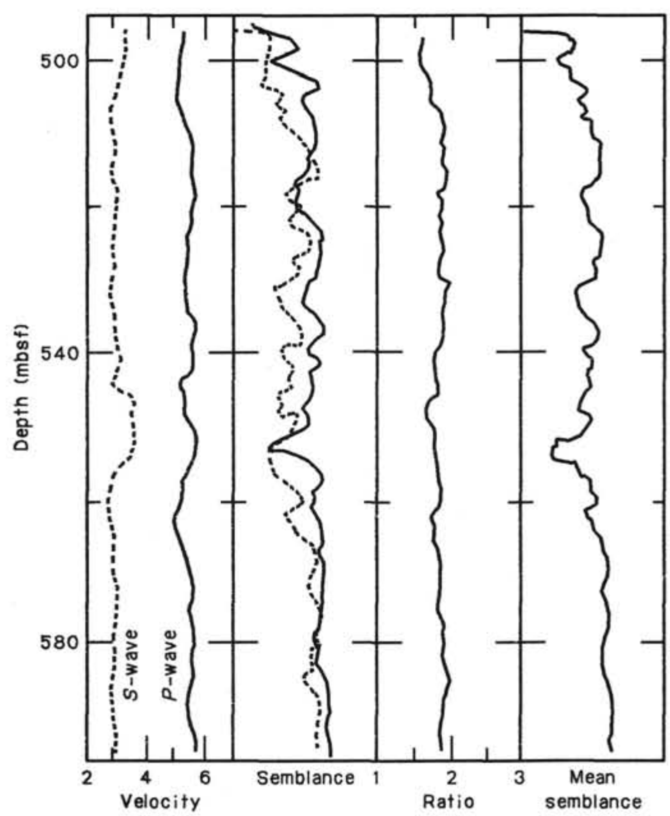

Figure 18. Compressional and shear velocities (km/s), semblances (from 0 to 1), velocity ratio, and mean semblance as a function of depth for the lowermost part of Hole 395A.

netic study of recovered rock samples from these holes and can provide data about the precise stratigraphic structure within the holes. In Hole 395A, the vertical component of the magnetic field was measured during Leg 78B (Ponomarev and Nechoroshkov, 1984). However, measurements of the three components of the magnetic field would provide more information about the nature of the young oceanic crust surrounding the hole. Therefore, magnetic-field measurements with the three-axis, gyroscope-controlled borehole magnetometer, which had been successfully used on Leg 102 (Salisbury, Scott, Auroux, et al., 1986), and a self-contained high-temperature three-axis borehole magnetometer, which has been newly developed in Japan, were included in the logging program on Leg 109. In this section, the the measurements with the two tools will be reported separately.

Three-Axis Gyroscope-Controlled Borehole Magnetometer

Instrumental Device and Performance of Measurement

This borehole magnetometer, which was developed by the Federal Institute for Geosciences and Natural Resources (BGR), Hannover, Federal Republic of Germany, basically comprises the following components:

1. A three-axis Foersterprobe fluxgate system, which measures the Earth's magnetic field in three mutually perpendicular directions, one parallel and two perpendicular to the borehole—sensitivity 1 nT.
2. A gradiometer, which measures the gradient of the magnetic field parallel to the borehole—sensitivity 2 nT/40 cm.
3. A directional unit, consisting of a gyroscope used as a directional reference (0.6°–1°/hr) and two inclinometers (accelerometers) with a sensitivity of 5×10^{-3} degree. This unit is fixed to the magnetometer, for which the position is, therefore, defined.
4. The electronic unit for signal processing, data transmission, and power supply.

Measurements are taken continuously downward and upward in the borehole (magnetometer log) and with the probe held stationary at discrete points at increments of 5–10 m. A detailed description of this borehole magnetometer is given by Bosum and Rehli (1985).

This magnetometer was successfully used on Leg 102. From the measurements, paleopole positions were calculable for the first time from ODP data. To suppress a probe rotation within the borehole from affecting the accuracy of determination of the declination, which was observed on Leg 102, a centralizer was developed for the magnetometer probe assembly and tested on Leg 109.

Hole 395A was logged with the BGR magnetometer on 5 June 1986. As the azimuth measurements show, the centralizing assembly yielded the expected suppression of the probe rotation. Hence, future magnetometer measurements with an improved accuracy are to be anticipated. Unfortunately, on Leg 109 we could not perform three-axis measurements because of damage to the three-axis fluxgate system, which was caused by a failure of the device connecting the centralizer with the magnetometer probe. (As verified by tests performed in a pressure chamber after the cruise, the device broke because of a reduction in material strength caused by an accumulation of stress near the thread, which is cut into the connector.) On Leg 109, only the vertical field was logged successfully with the gradiometer in the probe.

Results

Plate 2 (in back pocket) shows the vertical component of the magnetic field logged with the gradiometer on Leg 109. The most outstanding feature is the anomaly in the upper part of the log, where the magnetic intensity changes from about 21,000 nT to 31,000 nT, or from about −3800 nT to +6200 nT after subtraction of the regional field, which is estimated to be at 24,800 nT on the basis of the 1965 International Geomagnetic Reference Field (IGRF). This anomaly is caused by a reversal of the surrounding basalt units. Another less-developed anomaly was measured at the final depth of the downhole logging. The results of these measurements are characterized by high resolution and accuracy and by a high signal-to-noise ratio. The result of the measurements by the self-contained three-component magnetometer (Plate 2, in back pocket) agrees well with the result of Ponomarev and Nechoroshkov (1984) on Leg 78B.

Self-Contained High-Temperature Three-Axis Borehole Magnetometer

Instrument Description

This borehole magnetometer was specially designed for downhole measurements in ODP holes, where temperatures of as high as 300°C are expected within the region of young oceanic crust. The magnetometer is composed of a high-pressured vessel, which is made of MONEL alloy and which houses the measuring unit. This nonmagnetic MONEL alloy (magnetic permeability is 1.001) has a high tensile strength at high temperatures (no deterioration of strength up to 650°C). Therefore, the material is one of the best choices for the high-pressured vessel of the magnetometer. The thin, cylindrical magnetometer is 4.6 m long and 6.7 cm wide, which enables its use in almost all DSDP and ODP holes. Figure 19 shows a schematic drawing of the high-pressured vessel. For convenient carrying, the pressure vessel can be separated into four sections; the length of each section is about 1.2 m. Total weight of the magnetometer is about 100 kg.

To operate as a borehole magnetometer, these four sections are connected into one long cylinder. Water seal is attained by metal O-rings made of INCONEL or by rubber O-rings. Metal O-rings are used when a high temperature is expected. In Hole 395A, rubber O-rings were used since the maximum expected temperature was about 20°C. As shown in Figure 19, except in the bottom section which contains magnetic sensors and a temperature sensor, a thin metal tube is fitted inside the pressure vessel. The metal tube is supported by ceramic rings. The space between the outer pressure vessel and the inner tube, which is evacuated to a vacuum of 10^{-5} Torr, acts as a thermal insulator that prevents or delays thermal conduction from the outside of the magnetometer. This dewar system is not installed in the sensor because the sensor can sustain high temperatures up to 300°C.

This borehole magnetometer measures temperature and the three components of the magnetic field. A block diagram of the system is shown in Figure 20. Ring core fluxgate-type magnetic sensors are used for detecting the magnetic field. Three mutually perpendicular ring cores, drive coils, and pick-up coils are installed in the bottom section of the magnetometer. The mount of the pick-up coil and the supporter are made of ceramics, which ensure stability at high temperatures. As a temperature sensor, a platinum sensor (KTG-7) is used, which gives stable temperature readings compared with those of a thermistor. These sensors are installed near the lower end of the bottom section.

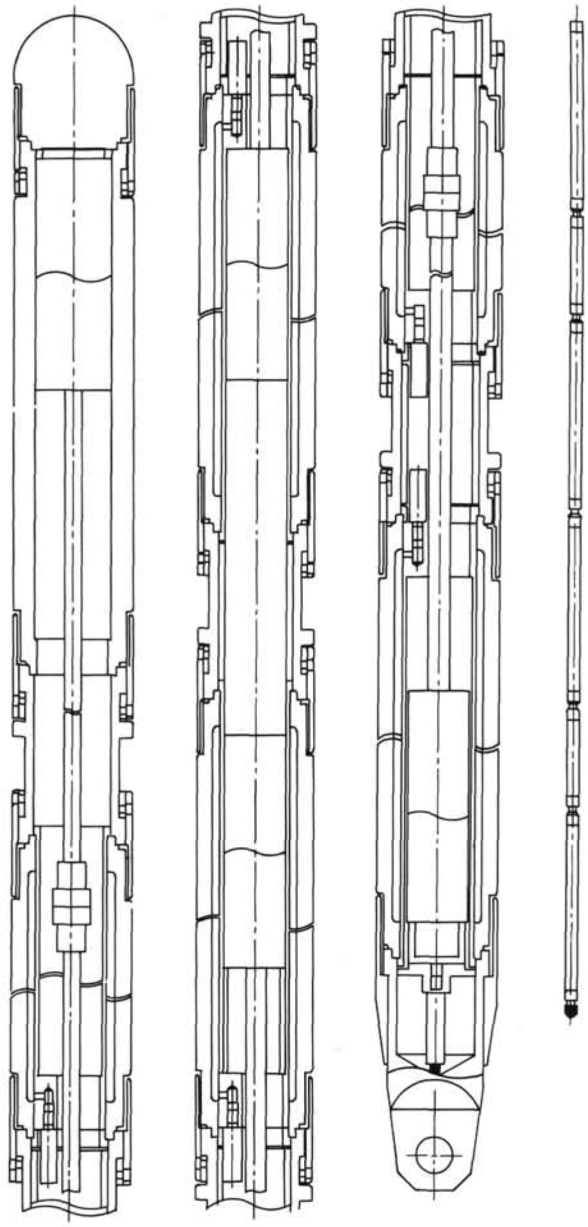

Figure 19. Schematic drawing of the high-pressured magnetometer vessel used on Leg 109.

The second section of the magnetometer houses the driving and the detection circuits for the magnetic sensors and the amplifier for the temperature sensor. The driving frequency of the fluxgate sensor is 15 kHz, and the detection circuit converts the amplitude of the first higher harmonics, which is proportional to the external field strength in the sensor direction, to the DC output voltage.

The third section contains four A/D converters for the three magnetic sensors and the temperature sensor. CMOS-type 17-bit A/D convertors (1 sign bit and 16 signal bits) are used where an extremely low drift and low noise reference voltage supply reduces the noise level to less than least significant bit (LSB). For magnetic measurement, the gain of the amplifier is adjusted so that the LSB corresponds to about 1 nT. Exact conversion factors, calibrated by a Helmholtz coil at the Kakioka Magnetic Observatory, Japan, are 1.10280, 1.10420, and 1.10486 nT/count for X, Y, and Z sensors, respectively. Because of the 17-bit A/D converter, the range of the measurable magnetic field is about ±65,000 nT, which is enough for most purposes. Although the sensitivity is carefully adjusted at room temperature, high temperature would change the sensitivity. Hence, a calibration current, which corresponds to the magnetic field of about 4900 nT, is applied in alternating directions for every two measurements of the magnetic field. This calibration signal can be used for the later adjustment of the actual sensitivity of the magnetic sensors. The range of the temperature measurement is from 0° to 300°C, and the output voltage at 300°C is adjusted to the maximum voltage for the A/D convertor (+5 V). Hence, the resolution of the temperature measurements becomes 0.0044°C/count, a precise measurement of the temperature. The timer and controller are also installed in this section. The timer can start the measurement after a specified time has elapsed, which is important for efficient measurements.

The digital signals from the A/D convertors are stored in IC memory, consisting of electrically erasable programmable read only memory (EEPROM). The maximum available memory space is 80 kbyte, which is supplied by ten 64-kbit memory chips. Since 12 bytes are required for each measurement (3 components of magnetic field and a temperature), one chip is enough for about 5 hr of measurement with a sampling rate of 30 s.

The top section contains a battery power source for the magnetometer. Twenty lithium batteries (National BR-2/3A) are used to supply voltages of +18V, −18V, and +9V. Because of the space limitation for the batteries, the maximum duration of the measurement is about 4.5 hr. In the future, this period should be extended. The battery box can be pulled out easily from the high-pressured vessel for battery exchanges by opening only the end cap of the magnetometer. Hence, the preparation time between successive runs is less than half an hour.

Besides the magnetometer, an on-board interface box is provided. This box gives external power to check the magnetometer and transfers control signals to the magnetometer. The box also contains an interface for the transfer of data from the magnetometer to a microcomputer for permanent storage and data reduction. At present, an EPSON HC-40 hand-held computer is used as a host computer.

Experiments

Downhole measurement of the magnetic field with this apparatus was made on 7 June 1986. This operation was combined with the MCS measurement. The magnetometer was hooked to the bottom of the MCS logging tool, and both apparatuses were lowered together by cable. The self-contained nature of the magnetometer (no cable for the power and signal transmission) enabled this combined experiment.

Just before the operation began, the magnetometer timer was started and the magnetometer was hooked to the MCS logging tool. The time was 1029 hr, and the specified delay time for the start of the measurements was 4 hr and 13 min. Lowering the combined tools started at 1100 hr from the rig floor and reached the bottom end of the drill pipe at 1300 hr (106 mbsf). Next, the downgoing MCS measurements were made at a logging speed of about 5 m/min. The tools reached the bottom of the hole at 1445 hr, which was almost exactly the time when the magnetometer started the measurements. The tools started logging uphole at 1454 hr at a speed of 2 m/min. Because the magnetometer measures the signal every 30 s, the sampling interval at this speed is 1 m. The speed was kept constant until the tools reached the bottom of the pipe at 1900 hr. The tools were then pulled up with the speed of about 2500 m/hr and were back on board just before 2100 hr. Because the timing of the operation

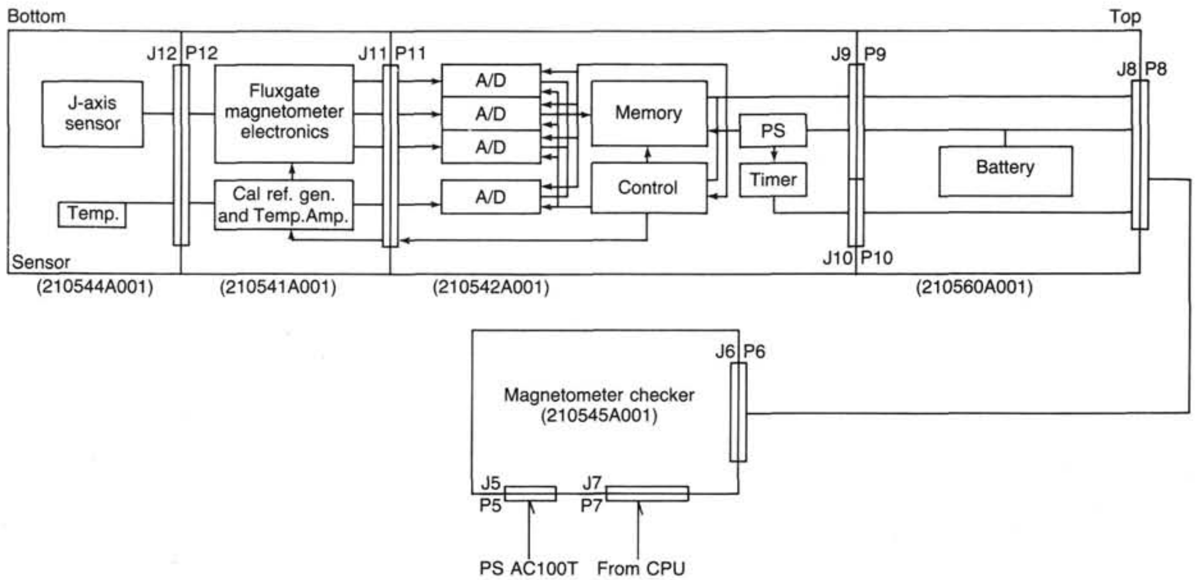

Figure 20. Block diagram of the magnetometer system.

was perfect, the measurement time of the magnetometer (4 hr and 30 min) was effectively used. After a few hours of waiting for the temperature to equilibrate to room temperature, we opened the magnetometer and transferred the data to the computer for analysis.

Results and Discussion

The magnetometer measured the three components of the magnetic field and the temperature within Hole 395A from 606 to 106 mbsf. The sampling rate and the sampling interval were 30 s and 1 m, respectively. For the on-board processing, only the data with a 1-min interval was used because another half of the data contains the calibration signal and requires some calculation. From the observed three components of the magnetic field, we calculated the magnetic total force, the horizontal component, the vertical component, and the inclination of the magnetic field inside the hole. Results are shown in Plate 2 (in back pocket) and Figure 21.

The variation of the vertical component of the magnetic field through Hole 395A is shown in Plate 2 (in back pocket). The vertical component can be compared with the Leg 78B result and the measurement made by the German magnetometer used during Leg 109, which measured only the vertical component. The most prominent feature in the variation of the vertical field is the sharp jumps observed at about 256 and 576 mbsf. At the lower jump, the vertical field increases; the field decreases at the upper jump. These features were observed during the magnetic logging of Leg 78B. The depths of the jumps are closely correlated with transitions of the magnetization of the basaltic rocks, which were observed from the paleomagnetic study of the rocks recovered from Hole 395A during Leg 45. Basalts recovered below 576 mbsf and above 256 mbsf are normally magnetized, and those between the two boundaries are reversely magnetized. The sense of the jump is consistent with the expected reversals. The offset value at the upper jump is much larger than at the lower one.

Besides the aforementioned jumps, the variation of the vertical component has high-frequency components, the approximate wave length being about 5 m. These features are consistent with the results from the German magnetometer logging during Leg 109. The same feature obtained by the different logs suggests that the high-frequency variation is real and represents the

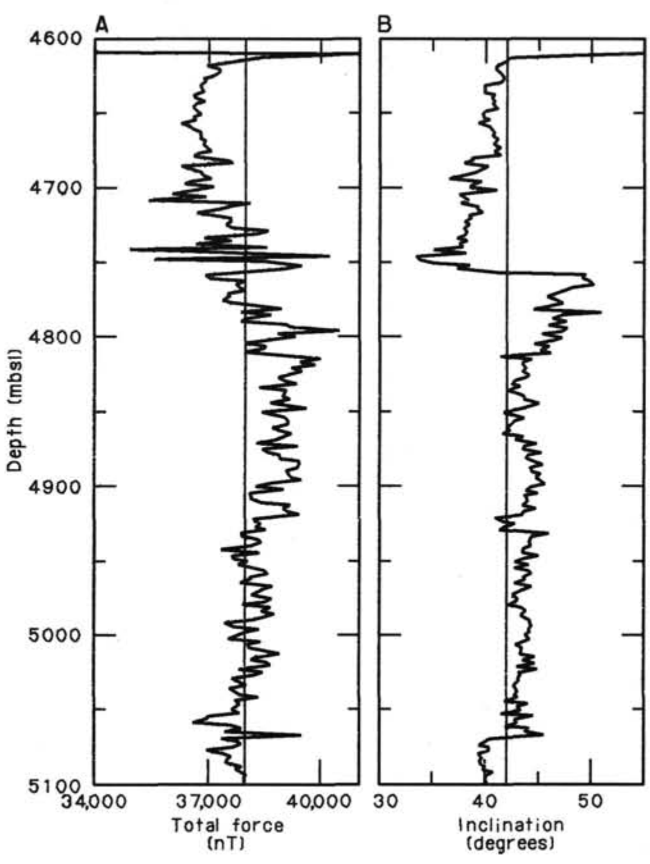

Figure 21. Depth variations of the magnetic total force (A) and the inclination (B) in Hole 395A.

actual variation of the magnetic field within this hole. Low-frequency variation of the signals shows a monotonous decrease of the vertical field with depth through the upper, normally magnetized section and the middle, reversely magnetized section. The average rate of the variation is about 100 nT/100 m.

The variation of the horizontal component is also shown in Plate 2. Abrupt changes of the horizontal component are also seen in this plate, although the directions of the jumps are opposite to the vertical component, which is also compatible with the interpretation based on the reversal of the magnetization of the surrounding material. The ratio of the offset values of the vertical component to the horizontal component can give information about the inclination of the normally magnetized and reversely magnetized sections. In contrast to the vertical component, the horizontal component does not show a monotonous variation with depth. Except for the depth range from 206 to 306 mbsf, the horizontal field intensity is mostly confined within ± 1000 nT of the mean value of 28,000 nT. The large deviation of the field value from the mean value is observed within ± 50 m of the upper transition point.

Conclusions

Three components of the magnetic field and the temperature were measured through Hole 395A with a self-contained borehole magnetometer. The observed distributions of the vertical component of the magnetic field and the temperature are consistent with the previous measurements. The present observation of the magnetic total force and the horizontal component of the magnetic field can give more precise information about the structure of young oceanic crust.

MAGNETIC-SUSCEPTIBILITY LOG

Magnetic-susceptibility logging measured in drill holes is a relatively new way to get information about the nature and the content of ferromagnetic minerals in deep rock formations. Magnetic susceptibility is an accurate measure of the abundance of ferromagnetic minerals such as magnetite, titanomagnetite, and pyrrhotite. In ocean-floor basalts, the dominant magnetic mineral is titanomagnetite, occurring in various concentrations and grain sizes. Because of the dependency of the susceptibility on grain size, the susceptibility log may distinguish coarse-grained basalts (massive flows with a low cooling rate) from fine-grained basalts (pillows with a high cooling rate). The general variation of the magnetic susceptibility with depth also provides information about the state and alteration of the ferromagnetic minerals in the rocks.

Description of the Susceptibility Tool

The magnetic-susceptibility tool, developed by the Institute of Applied Geophysics at the University of Munich, is similar to an induction-logging tool (Fig. 22). It consists of three vertically oriented coils at the bottom part of the device placed inside a nonconductive pressure barrel, which is made of a ceramic tube surrounded by fiberglass-reinforced epoxy resin for shock absorption. The spacing between transmitter coil and receiver coil is 40 cm. A power amplifier supplies the transmitter coil with constant AC current at a frequency of 1000 Hz. The quadrature oscillator puts out two voltages with 90° phase shifts. The in-phase voltage drives the output amplifier and triggers the in-phase detector, and the 90° phase-shifted voltage triggers the quadrature detector. The directly induced voltage in the receiver coil, corresponding to zero susceptibility, is compensated by the voltage induced in a small coil near the transmitter coil. The resulting signal is preamplified and run through a band-pass filter to suppress higher harmonics of the main frequency.

The outputs of the two phase-sensitive detectors are, as determined by a first-order approximation, proportional to the magnetic susceptibility and the electrical conductivity of the surrounding material. The higher order terms show that the susceptibility signal and the conductivity are mutually dependent. Recording both voltages, the in-phase and the quadrature part, permits a correction of the susceptibility of highly conductive surrounding media. This is an important advantage for use in situations where the borehole fluid is saltwater, as in ODP drill holes. Normally, logs measured in drill holes with highly resistive drilling fluid have to be corrected only by a caliper factor to get the true susceptibility value.

Borehole Conditions

Because the principle of the magnetic-susceptibility measurement is based on the induction between two coils, it is important to know the exact diameter of the borehole and the conductivity of the borehole fluid for corrections. Although Hole 395A was drilled with an 8¾-in. bit (22.23 cm), the average borehole diameter is approximately 30 cm (Melson, Rabinowitz, et al., 1979).

From caliper measurements in Hole 395A on Leg 78B (Mathews et al., 1984), it can be seen that the diameter varies between 28 and 48 cm (maximum tension of the caliper tool). Beneath small spikelike changes of the diameter, the caliper log also shows caves and washouts having diameters of up to 40 cm and lengths of more than 10 m. These cavings falsify the susceptibility log in two ways. In sections with larger diameters, the signal normally will decrease. If highly conductive fluid is in the hole, however, the signal will increase in the sections of larger diameter because of an increase in the higher conductive volume around the probe.

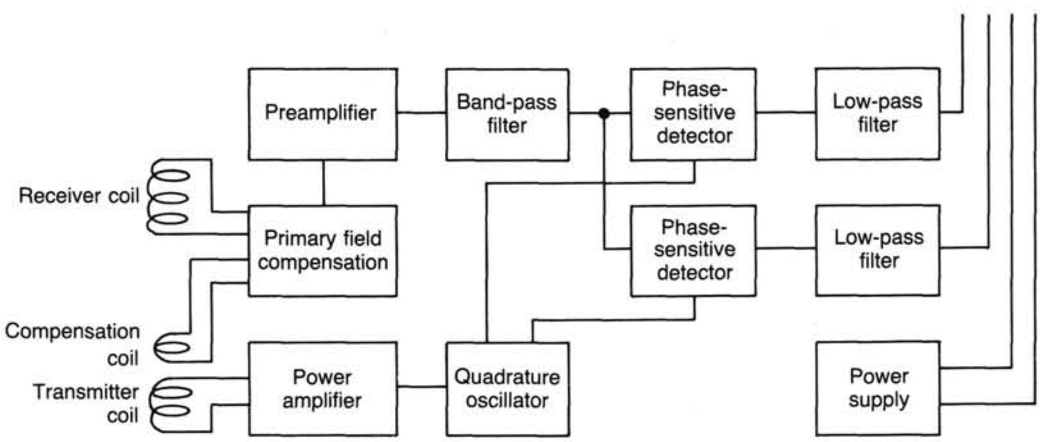

Figure 22. Electronic blocks of the magnetic-susceptibility tool developed at the University of Munich.

Results

The susceptibility logging (Plate 2, in back pocket) was conducted on 7 June 1986 and lasted 10 hr, including the runs through the pipe. Logging speed downhole was 10 m/min and 5 m/min uphole. Susceptibility and conductivity signals were digitized every 10 cm. The depth indicated by the counter on the winch has to be corrected with the actual depth of the casing shoe, which causes a full-scale change in the signal amplitude. Figure 23 shows the upward-recorded susceptibility log, the lithostratigraphy of Hole 395A, and the susceptibility measured on core samples (Johnson, pers. comm., 1986). The log was

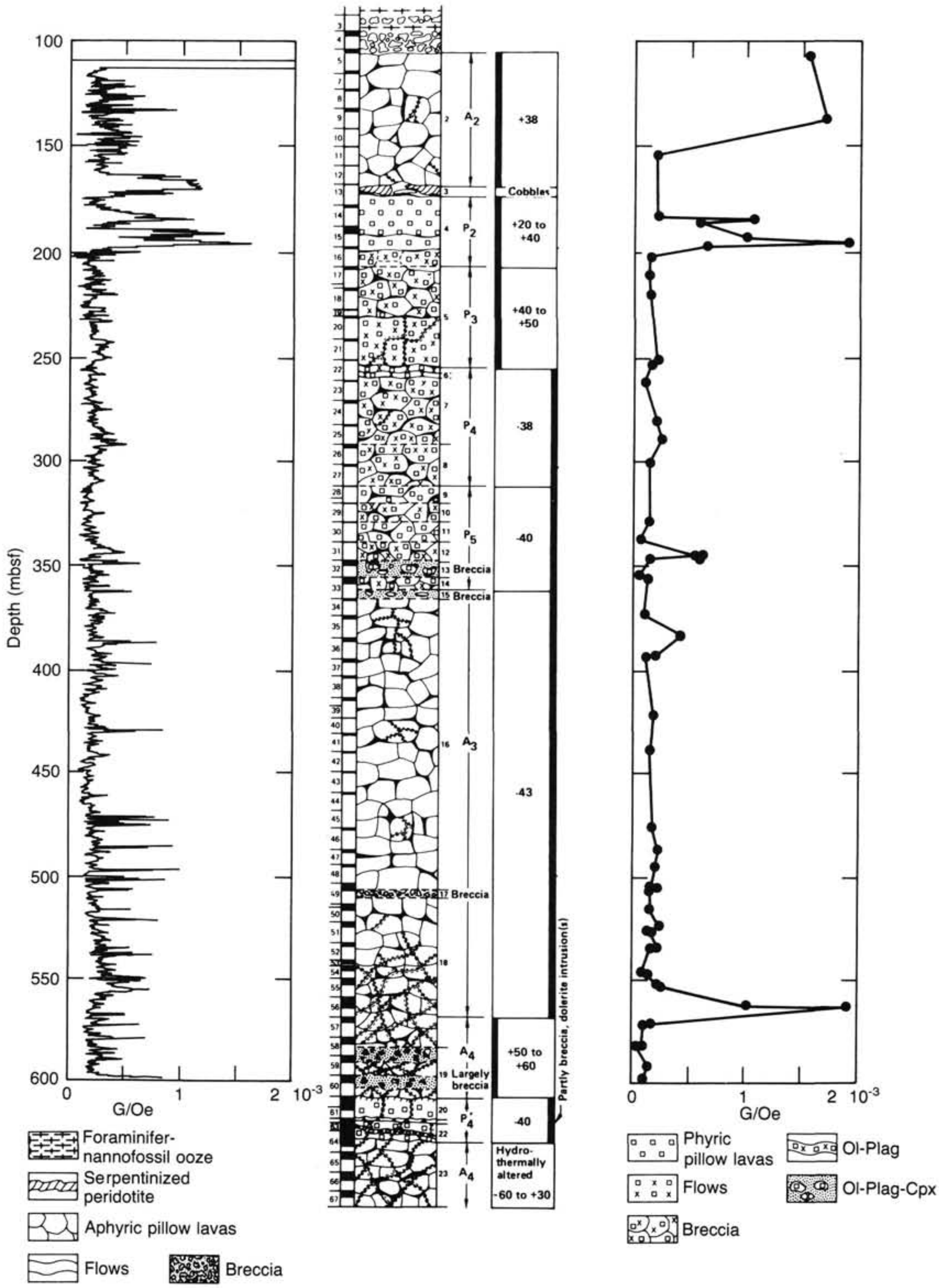

Figure 23. Magnetic-susceptibility log, lithostratigraphy, and susceptibility as measured on core samples from Hole 395A. Lithology from Melson, Rabinowitz, et al. (1979).

smoothed by glide averaging with a length of 50 cm. On the basis of the 40-cm spacing between the receiver and transmitter coil, the bed resolution is about 30–40 cm. The influence of the highly conductive borehole fluid was reduced by subtracting a fraction of the conductivity signal from the recorded susceptibility log.

The two susceptibility measurements (Fig. 23) correlate well in amplitude and depth. The massive basalt unit 4 and the breccia zone between 340 and 350 mbsf can be easily recognized in both logs. The uppermost maxima of the susceptibility log is caused by the serpentinized peridotites, which were recovered from a depth of 172.5–174.3 mbsf, as described in the site summary of Leg 45 (Melson, Rabinowitz, et al., 1979). Titanium-free magnetite resulting from high-temperature alteration causes the high susceptibility values (Johnson, 1978a). The next lower maxima can be attributed to massive basalts (Hole 395A, Cores 14 and 15, DSDP Leg 45) having the larger grain sizes (20–100 μm) of the titanomagnetites (Johnson, 1978a). As indicated by the Russian scientists on Leg 78B (Ponomarev and Nechoroshkov, 1984), further serpentinites between 175 and 200 mbsf could also occur because of the similarity of the maxima in the susceptibility log. The peak in the depth of 345 mbsf is caused by a carbonate-cemented breccia zone (Hole 395A, Core 32, DSDP Leg 45) having low-titanium magnetite grains that contain ilmenite lamellae (Johnson, 1978b). Like the serpentinized peridotites, this breccia zone has been exposed to high-temperature alteration.

The most conspicuous aspect of this log is the uniformity from a depth of 200 mbsf to the bottom. The susceptibility log measured on Leg 78B (Ponomarev and Nechoroshkov, 1984) shows a similar behavior, except for the anomalous bulge at 430 mbsf. Such uniformity over such great depth is not normal; most susceptibility logs measured in basalts show much more variation and structure. The uniformity of the Leg 109 log and the relatively small susceptibility can be explained by the grain sizes of the titanomagnetites. Between 200 and 600 mbsf, most grain sizes of the opaque minerals measured from 28 samples (Johnson, 1978b) are <20 μm. Only one sample from a depth of 301 mbsf shows grains as large as 50 μm. Contrasting to this, grain sizes of the opaques of three samples from between 180 and 200 mbsf are between 20 and 100 μm. The average susceptibility value of the uniform part of the log is 0.2×10^{-3} G/Oe, which is based on a borehole diameter of 30 cm. Compared with the average value of the susceptibility log measured on Leg 78B, this value is lower. The average value for the pillow basalts given by Johnson (1978a) is 0.17×10^{-3} G/Oe.

With increasing depth, more spikes can be seen in the log. Especially from 470 to 600 mbsf, the great number of spikes can be attributed to an increase of the abundance of rocks containing fractures filled with secondary minerals (Melson, Rabinowitz, et al., 1979). Pyrrhotite as a relict of water-circulating systems in these fractures could cause the spikes. This correlates with the temperature-gradient log (Plate 2, in back pocket), which indicates water circulation at depths of 430 and 470 mbsf, where large changes of the temperature gradient can be correlated with spikes in the susceptibility log.

In summary, the susceptibility log measured in Hole 395A shows a clear dependency on the grain size of the titanomagnetites in the basalts. Coarse-grained massive basalts can be easily distinguished in the log from fine-grained pillows. Compared with the massive basalts, the serpentinized peridotites (163–173 mbsf) also have high but more homogeneous susceptibility. Especially for this stratigraphic unit, the clear occurrence in the susceptibility log allows an exact determination of depth and thickness, which agrees better with the stratigraphy of Hole 395.

HYDROGEOLOGY EXPERIMENTS IN HOLE 395A—LARGE-SCALE RESISTIVITY AND PACKER TESTS

Circulation of seawater through fresh basalt greatly affects the development of the physical and chemical nature of the oceanic crust. The modes and effects of circulation are partly controlled by the variable permeability and porosity of the basaltic layer. Because these crustal parameters probably vary with irregular fractures and voids of unknown scale, they cannot be reliably determined from dredged or cored samples. Instead, independent measurements of bulk porosity are essential in relating the physical properties measured on recovered samples to the formation properties of the crust. Bulk permeability and porosity must be measured *in situ*, at average scales large enough to include the effects of irregular fracture porosity and to exclude the effects of drilling disturbance on the formation.

Deep boreholes offer perhaps the best opportunities to measure bulk porosity and permeability *in situ*; two special experiments were run during Leg 109 to measure these properties in Hole 395A: the large-scale electrical-resistivity, and the formation tests using a drill-string packer. Because the electrical conductivity of the pore fluids (essentially seawater) is several orders of magnitude greater than the conductivity of basalt, measurements of the electrical resistivity of the formation over a large scale are sensitive to the bulk porosity. The bulk permeability is related in a complicated way to interconnected porosity and was measured after isolating sections of the formation using an inflatable rubber packer.

During Leg 109, the large-scale resistivity experiment was successfully run throughout the open-hole section of Hole 395A, and a packer was successfully set at 210 and 80 m above the bottom of the hole, allowing bulk permeability to be measured over the depth intervals of 396–606 and 526–606 mbsf. In addition, detailed analysis of temperatures measured at Site 395 will yield an estimate of the bulk permeability of the uppermost 300–400 m of basement in the hole.

Large-Scale Resistivity Experiment

The large-scale resistivity experiment, first deployed on Leg 60 by Francis (1982), who discussed the methods in detail, was run twice in Hole 504B, first during Leg 70 to 836 mbsf (Von Herzen et al., 1983) and again during Leg 83 to 1287.5 mbsf (Becker et al., 1982; Becker, 1985). The experiment is a simple, long-spaced DC resistivity log, as diagrammed in Figure 24. A large current is passed from the ship down the armored logging cable through an insulated cable to a steel sinker-bar/current-electrode. The current then returns through the formation and the seawater back to the ship. Despite the high conductivity of seawater in the borehole, the long, narrow return path up the borehole is relatively resistive (about 5 Ω/m), so that the current may be assumed to return through the formation. In response to the resistivity of the formation, a potential gradient is set up in the borehole, and it is sampled with several nonpolarizing Ag/AgCl electrodes mounted above the current electrode.

The Leg 109 experiment in Hole 395A was run just like the Leg 83 experiment in Hole 504B (Becker et al., 1982; Becker, 1985). Four potential electrodes were spaced 10, 20, 40, and 80 m above the current electrode, and a 300-V power supply passed currents of 3.4–4.0 A through the formation. The experiment was run at discrete, stationary intervals: at each level, current was passed for about 10 s each under positive and reversed voltage. This allows removal by averaging of any biases between electrodes arising from possible ambient potential gradients in the hole. The hole was logged in 10-m increments, with the

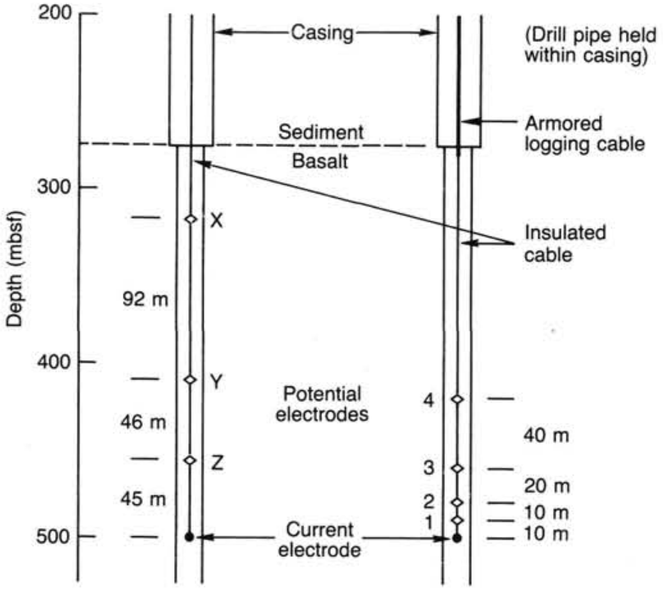

Figure 24. Downhole configurations for the large-scale resistivity experiments run in Holes 395A and 504B. The Leg 109 experiment in Hole 395A was run using the configuration on the right. Loggings at X, Y, Z, and 1-4 show location of the potential electrodes.

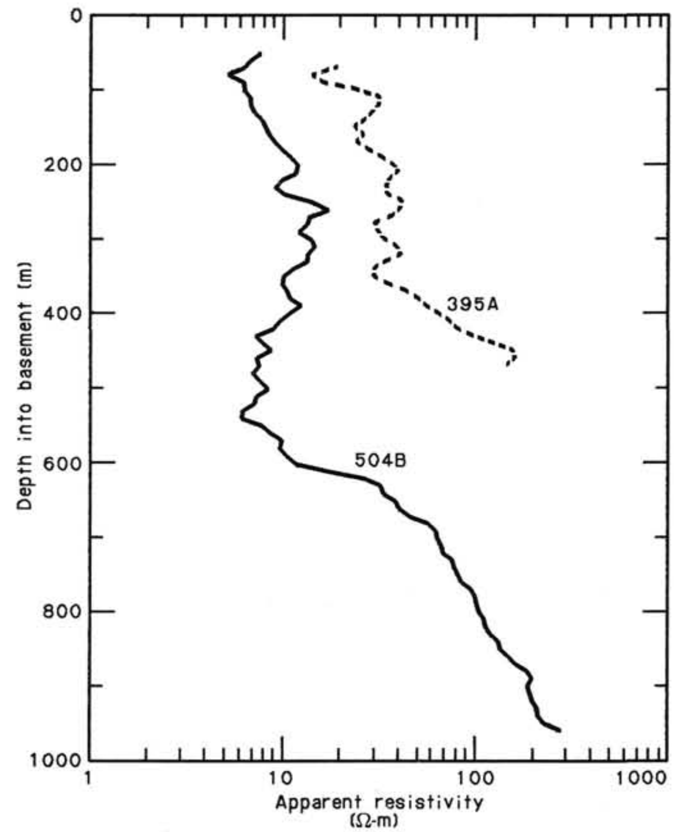

Figure 25. Apparent resistivities in Holes 395A and 504B, calculated from voltage differences measured using electrode pair 3-4.

sinker-bar between 600 and 130 mbsf. Potential differences were recorded for four different electrode pairs, 1-2, 2-3, 3-4, and 1-4, which respond to bulk resistivities averaged over vertical and radial scales of about 5-50 m from the borehole. The redundant data are of very good quality; at every depth, the sum of the smaller interval voltages duplicates the greatest interval voltage to well within 1%.

Measured voltages range over three orders of magnitude, indicating a large range for the bulk resistivities, as occurred in Hole 504B. *In-situ* resistivities were approximated by calculating apparent resistivities from measured voltages, using the exact solution for the potential that arises from a point current source in a borehole that penetrates a homogeneous medium (equations 2 and 3 of Becker, 1985). Figure 25 shows apparent resistivities in both Holes 395A and 504B calculated from the voltage differences recorded by electrode pair 3-4, which responded to *in-situ* resistivities averaged vertically and to radial scales on the order of 20-40 m from the borehole. A similar but noisier range in resistivities is shown by the Schlumberger SFL (Plate 1, in back pocket), which probes much shallower into the formation (about 0.5 m).

Permeability Tests Using a Drill-String Packer

A packer can be simply defined as a device that produces a hydraulic seal in a borehole (Fig. 26). If this hydraulic seal is properly maintained, the hydrologic properties of the formation can be tested by applying differential fluid pressures to the isolated section. Formation properties that can be measured using a packer include pore pressure, transmissivity (from which permeability can be derived), and storage coefficient (which is closely related to bulk formation porosity). These properties are determined from measurements of pressure in the isolated section during two types of tests:

1. Pulse tests are those in which downhole-pressure recorders monitor the decay of short, effectively instantaneous pressure pulses applied to the formation using the surface pumps. In a relatively impermeable formation, the period of decay of such a pulse will be long compared with the duration of the pulse, and the permeability can be determined using the theory for an instantaneous pulse. In a permeable formation, a pressure pulse will decay rapidly, and flow tests must be run.

2. Constant flow tests are those in which downhole-pressure recorders monitor the approach of downhole pressure to a constant value as fluid is pumped into the formation at a constant rate. If a steady state is reached, the permeability can be estimated using a form of Darcy's Law.

During Leg 109, a drill-string packer manufactured by TAM International (described by Becker, 1986) was successfully inflated at two positions in Hole 395A: (1) at 396 mbsf, for measurement of bulk permeability over the interval of 396-606 mbsf, and (2) at 526 mbsf, for determination of bulk permeability over the interval of 526-606 mbsf. These two inflation positions were chosen from the televiewer and caliper-log data of Hickman et al. (1984b), which indicated relatively narrow and smooth hole conditions at these depths. The packer was configured as a short straddle packer, with two inflatable elements approximately 1 m apart; however, it was used as a single-element packer to isolate the section of borehole below the packer. If time had allowed, the straddle packer might have been used in its straddle capacity, to try to hydrofracture a short section of borehole isolated between the two inflatable elements.

At each inflation depth, the formation below the packer was tested by monitoring pressures with two downhole mechanical pressure gauges (Kuster K-3 gauges). Similar test procedures were followed at each depth; several pulse tests of 500-1250-psi amplitude were run, but the periods of decay of these pulses were very short. Constant flow tests were then attempted by pumping at rates of 2-3 bbl/min for roughly 30 min, when measured

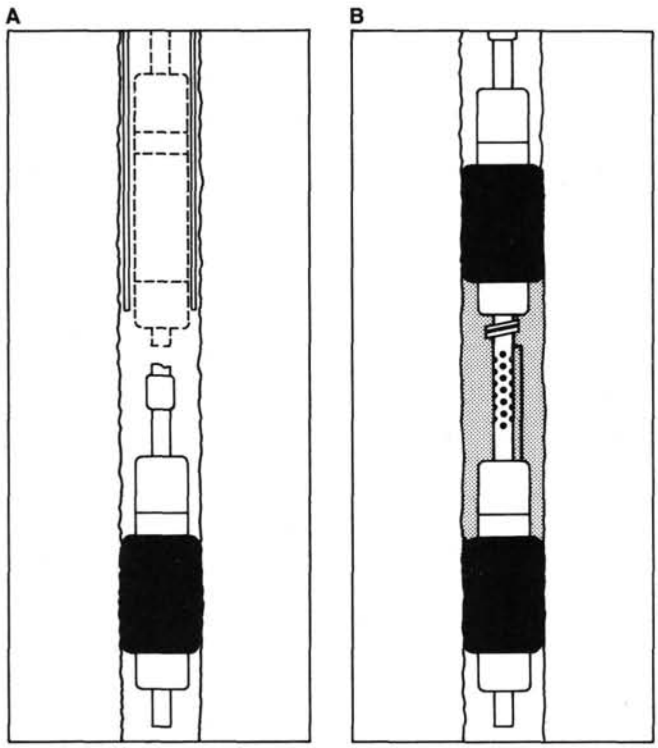

Figure 26. Sketches of inflatable drill-string packers. A. Single-element packer, which isolates the formation between the element and the bottom of the hole. B. Straddle packer, which separately isolates the zone between the elements and the zone between the lower element and the bottom of the hole.

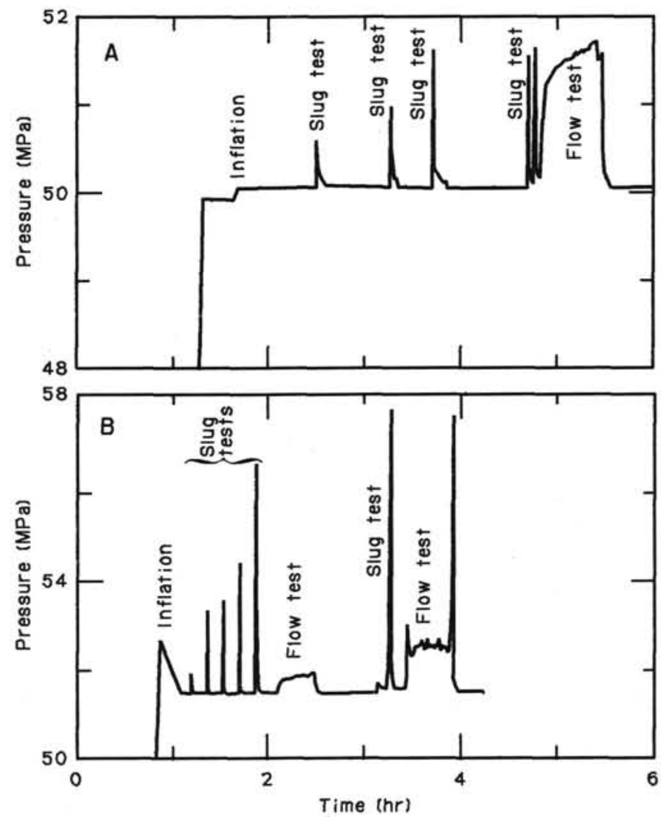

Figure 27. Pressure-time records of the two Leg 109 packer settings in Hole 395A: A. 396 mbsf. B. 526 mbsf.

pressures came to nearly constant values of 100–300 psi above hydrostatic levels. The analog records produced by the Kuster pressure recorders are shown in Figure 27. The records are of very good quality and have excellent drill-string heave compensation; there are none of the noisy oscillations caused by heave that marked many of the records obtained in packer tests run on DSDP legs.

Leg 109 pressure records will require careful processing to determine the permeability of the crust penetrated by Hole 395A. Preliminary analyses indicate that the results will be significantly different from the extremely low permeability measured in the interval below 583 mbsf during Leg 78 by Hickman et al. (1984a). A packer was set during Leg 78B in a massive unit at the bottom of the hole, and the permeability of this unit was determined from the slow decay of a pressure pulse. During the Leg 109 tests, all pressure pulses decayed quickly, necessitating flow tests and suggesting that the permeability in the tested intervals is much greater than that in the massive unit at the base of the hole, probably by orders of magnitude. In addition, the temperature measurements indicate a strong downhole flow of ocean-bottom water into the uppermost 300 m of basement, suggesting significant permeability in the section above the intervals tested during Leg 109.

Thus the preliminary Leg 109 packer results indicate that most of the section cored in Hole 395A has a very high permeability, on the order of or greater than the permeability of 10^{-13} m^2 measured in layer 2A in Hole 504B (Anderson and Zoback, 1982; Becker et al., 1983b). In contrast to Hole 504B, where much of the pillow-lava section is sealed and relatively impermeable, most of the lava pile in Hole 395A appears to be highly permeable and still open to extensive hydrothermal circulation.

REFERENCES

Anderson, R. N., Honnorez, J., et al., 1982. DSDP Hole 504B, the first reference section over 1 km through layer 2 of the oceanic crust. *Nature*, 300:589–594.

Anderson, R. N., Honnorez, J., Becker, K., et al., 1985. *Init. Repts. DSDP*, 83: Washington (U.S. Govt. Printing Office).

Anderson, R. N., and Zoback, M. D., 1982. Permeability underpressures, and convection in the oceanic crust near the Costa Rica Rift, eastern equatorial Pacific. *J. Geophys. Res.*, 87:2860–2868.

Anderson, R. N., Zoback, M. D., Hickman, S. H., and Newmark, R. L., 1985. Permeability versus depth in the upper oceanic crust: in situ measurements in DSDP Hole 504B, eastern equatorial Pacific. *J. Geophys. Res.*, 90:3659–3669.

Becker, K., 1985. Large-scale electrical resistivity and bulk porosity of the oceanic crust, Deep Sea Drilling Project Hole 504B, Cost Rica Rift. *In* Anderson, R. N., Honnorez, J., Becker, K., et al., *Init. Repts. DSDP*, 83: Washington (U.S. Govt. Printing Office), 419–427.

———, 1986. Special report: development and use of packers in ODP. *JOIDES J.* 12(2):51–57.

Becker, K., Langseth, M. G., and Hyndman, R. D., 1984. Temperature measurements in Hole 395A, Leg 78B. *In* Hyndman, R. D., Salisbury, M. H., et al., *Init. Repts. DSDP, 78B*: Washington (U.S. Govt. Printing Office), 689–698.

Becker, K., Langseth, M. G., and Von Herzen, R. P., 1983a. Deep crustal geothermal measurements, Hole 504B, Deep Sea Drilling Project Legs 69 and 70. *In* Cann, J. R., Langseth, M. G., Honnorez, J., Von Herzen, R. P., White, S. M., et al., *Init. Repts. DSDP*, 69: Washington (U.S. Govt. Printing Office), 223–235.

Becker, K., Langseth, M. G., Von Herzen, R. P., and Anderson, R. N., 1983b. Deep crustal geothermal measurements, Hole 504B, Costa Rica Rift. *J. Geophys. Res.*, 88:3447–3457.

Becker, K., Von Herzen, R. P., Francis, T.J.G., et al., 1982. In situ electrical resistivity and bulk porosity of the oceanic crust, Costa Rica Rift. *Nature*, 300:594–598.

Bosum, W., and Rehli, H. J., 1985. Bau und Erprobung eines 3-D-Bohrlochmagnetometers. *Geol. Jahrb.*, E28, Hannover, 191-217.

Cann, J. R., Langseth, M. G., Honnorez, J., Von Herzen, R. P., White, S. M., et al., 1983. *Init. Repts. DSDP*, 69: Washington (U.S. Govt. Printing Office).

Francis, T.J.G., 1982. Large-scale resistivity experiment at Deep Sea Drilling Project Hole 459B. *In* Hussong, D. M., Uyeda, S., et al., *Init. Repts. DSDP*, 60: Washington (U.S. Govt. Printing Office), 841-852.

Hickman, S. H., Langseth, M. G., and Svitek, J. F., 1984a. *In situ* permeability and pore-pressure measurements near the Mid-Atlantic Ridge, Deep Sea Drilling Project Hole 395A. *In* Hyndman, R. D., Salisbury, M. H., et al., *Init. Repts. DSDP*, 78B: Washington (U.S. Govt. Printing Office), 699-708.

Hickman, S. H., Svitek, J. F., and Langseth, M. G., 1984b. Borehole televiewer log of Hole 395A. *In* Hyndman, R. D., Salisbury, M. H., et al., *Init. Repts. DSDP*, 78B: Washington (U.S. Govt. Printing Office). 709-715.

Hyndman, R. D., Salisbury, M. H., et al., 1984. *Init. Repts. DSDP*, 78B: Washington (U.S. Govt. Printing Office).

Jaegar, J. C., 1942. Heat flow in the region bounded internally by a circular cylinder. *R. Soc. Edinburgh Proc.*, A, 61:223-228.

Johnson, H. P., 1978a. Rock magnetic properties of igneous rock samples—Leg 45. *In* Melson, W. G., Rabinowitz, P. D., et al., *Init. Repts. DSDP*, 45: Washington (U.S. Govt. Printing Office), 397-406.

________, 1978b. Opaque mineralogy of the igneous rock samples from DSDP Hole 395A. *In* Melson, W. G., Rabinowitz, P. D., et al., *Init. Repts. DSDP*, 45: Washington (U.S. Govt. Printing Office), 407-420.

Kopietz, J., 1984. Implications of thermophysical properties in geoscientific investigations for the disposal of nuclear waste in a salt dome. *High Temp.-High Pressures*, 16:67-79.

Lister, C.R.B., 1977. Estimators for heat flow and deep rock properties based on boundary layer theory. *Tectonophysics*, 41:157-171.

Mathews, M., Salisbury, M. H., and Hyndman, R., 1984. Basement logging on the Mid-Atlantic Ridge, Deep Sea Drilling Project Hole 395A. *In* Hyndman, R. D., Salisbury, M. H., et al., *Init. Repts. DSDP*, 78B: Washington (U.S. Govt. Printing Office), 717-730.

Melson, W. G., Rabinowitz, P. D., et al., 1979. *Init. Repts. DSDP*, 45: Washington (U.S. Govt. Printing Office).

Moos, D., Goldberg, D., Hobart, M. A., and Anderson, R. N., 1986. Elastic wave velocities in layer 2A from full waveform sonic logs at Hole 504B. *In* Leinen, M., Rea, D. K., et al., *Init. Repts. DSDP*, 92: Washington (U.S. Govt. Printing Office), 563-570.

Parsons, B., and Sclater, J. G., 1977. An analysis of the variation of ocean floor bathymetry and heat flow with age. *J. Geophys. Res.*, 82:803-827.

Ponomarev, V. N., and Nechoroshkov, V. L., 1984. Downhole magnetic measurements in oceanic crustal Hole 395A on the Mid-Atlantic Ridge. *In* Hyndman, R. D., Salisbury, M. H., et al., *Init. Repts. DSDP*, 78B: Washington (U.S. Govt. Printing Office), 731-739.

Salisbury, M. H., and Hyndman, R. D., 1984. Leg 78B: Background, objectives, and geological setting. *In* Hyndman, R. D., Salisbury, M. H., et al., *Init. Repts. DSDP*, 78B: Washington (U.S. Govt. Printing Office), 635-652.

Salisbury, M. H., Scott, J. H., Auroux, C. A., et al., 1986. *Proc., Init. Repts. (Pt. A), ODP*, 102.

Schreiber, E., and Rabinowitz, P. D., 1978. Acoustic wave velocity measurements of oceanic crustal samples—DSDP, Leg 45. *In* Melson, W. G., Rabinowitz, P. D., et al., *Init. Repts. DSDP*, 45: Washington (U.S. Govt. Printing Office), 383-386.

Von Herzen, R. P., Francis, T.J.G., and Becker, K., 1983. *In situ* large-scale electrical resistivity of ocean crust, Hole 504B. *In* Cann, J. R., Langseth, M. G., Honnorez, J., Von Herzen, R. P., White, S. M., et al., *Init. Repts. DSDP*, 69: Washington (U.S. Govt. Printing Office), 237-244.